The Boundary Element Method Applied to the Solution of the Anomalous Diffusion Problem

José Antonio Marques Carrer[*] Mohammed Seaid[†] Jon Trevelyan[‡] Bruno dos Santos Solheid[§]

Abstract

A Boundary Element Method formulation is developed for the solution of the two-dimensional anomalous diffusion equation. Initially, the Riemann-Liouville Fractional derivative is applied on both sides of the partial differential equation (PDE), thus transferring the fractional derivatives to the Laplacian. The boundary integral equation is then obtained through a Weighted Residual formulation that employs the fundamental solution of the steady-state problem as the weighting function. The integral contained in the Riemann-Liouville formula is evaluated assuming that both the variable of interest and its normal derivative are constant in each time interval. Five examples are presented and discussed, in which the results from the proposed formulation are compared with the analytical solution, where available, otherwise with those furnished by a Finite Difference Method formulation. The analysis shows that the new method is capable of producing accurate results for a variety of problems, but small time steps are needed to capture the large temporal gradients that arise in the solution to problems governed by PDEs containing the fractional derivative $\partial^\alpha u/\partial t^\alpha$ with $\alpha < 0.5$. The use of the steady-state fundamental solution presents no hindrance to the ability of the new formulation to provide accurate solutions to time-dependent problems, and the method is shown to outperform a finite difference scheme in providing highly accurate solutions, even for problems dominated by conditions within the material and remote from the domain boundary.

Keywords. Boundary Element Method; Riemann-Liouville Fractional derivative

1 Introduction

Fractional calculus is as old as standard calculus, its accepted origin dating back to 1695, when a mention of fractional derivatives appears in the correspondence exchanged between Leibnitz and L'Hôpital: a historical survey can be found, for instance, in Miller and Ross [1] and Ortigueira [2]. The next major developments were in the 19th century, with contributions from renowned mathematicians, including Laplace, Fourier, Abel, Liouville and Riemann.

Many applications of fractional calculus may be found in the literature. Examples include modelling the transmission and spread of the Zika virus in Brazil and internationally to 32 countries [3], the vibration analysis of a beam or plate resting on a viscoelastic soil foundation [4], and the simulation of solute transport through porous media [5]. A recent survey of these, and many more, applications can be found in Sun et al. [6]. Accurate and reliable numerical tools for solving these kinds of problems have also become necessary. Finite Difference Method (FDM) formulations are commonly used, and these are seen, for instance, in Meerschaert and Tadjeran [7], Murilo and Yuste [8], Li et al. [9], Çelic and Duman [10], Li and Li [11], Sousa and Li [12], Tadjeran and Meerschaert [13], Murio [14] and Youste and Acedo [15]. Finite Element

[*]UFPR-Federal University of Paraná, Postgraduate Program in Numerical Methods in Engineering. Curitiba, Paraná, Brasil
[†]Department of Engineering, University of Durham, South Road, Durham DH1 3LE, UK
[‡]Department of Engineering, University of Durham, South Road, Durham DH1 3LE, UK
[§]UFPR-Federal University of Paraná, Curitiba, Paraná, Brasil

Method (FEM) formulations are rather less common; among them are Agrawal [16], Zheng et al. [17], Deng [18], Roop [19], and Huang et al. [20]. Few works deal with Boundary Element Method formulations. Dehghan and Safarpoor [21] used a dual reciprocity BEM formulation, and Katsikadelis [22] employed the concept of an analog equation together with the BEM to solve two-dimensional fractional differential equations. In Zafarghandi et al. [23] and Shirzadi et al. [24] other interesting approaches are used, involving radial basis functions and a meshless formulation.

The anomalous diffusion problem is no longer Brownian and cannot be described by a second-order diffusion equation (see, for instance, Yuste and Acedo [15]). Instead, it is described by a partial differential equation that contains a fractional time derivative of order α, $0 < \alpha < 1$, instead of the usual first order time derivative. The fractional differential operators are non-local, which means that when solving such problems, the determination of a future state of the system depends on the current and previous states; that is, it depends on the history. This aspect is quite similar to some time-dependent BEM formulations, e.g. Mansur [25], Wrobel [26]. To solve the anomalous diffusion equation in 2D, a novel BEM formulation is developed in this work. The formulation employs the fundamental solution related to the steady-state problem, i.e. that related to the Laplacian operator. Consequently, the resulting formulation is of the type D-BEM, with D indicating domain, as the basic BEM equation includes a domain integral term containing the time derivative of the variable of interest. To avoid dealing directly with the fractional derivative, represented here by the Caputo derivative [2], an inverse operation is performed using the Riemann-Liouville operator, thus replacing the fractional time derivative by an ordinary derivative and transferring the fractional derivative to the second order spatial derivatives. After doing so, a weighted residual equation is developed, in which the Riemann-Liouville operator appears under both domain and boundary integrals. As a consequence of evaluating the integral presented in the Riemann-Liouville operator, the solution of the problem for a specific value of time, say t_{n+1}, requires that all the previous values of the variables, up to the previous time t_n, must be taken into account, constituting the 'history contribution' of the analysis. This procedure is explained in detail in the following sections. It is important to note that when $\alpha = 1$, one obtains the standard BEM formulation, without the requirement for a history contribution.

The formulation presented here could be called FD-BEM, with F meaning fractional, only to distinguish it from the standard one. In this way, the D-BEM formulation is treated as a particular case of the FD-BEM formulation, for which $\alpha = 1$. In the text, for practical purposes, the results obtained by the FD-BEM formulation will be referred to simply as BEM results.

Five examples are presented showing the performance of FD-BEM. The results are compared against analytical solutions where they are available, otherwise we use reference solutions taken from refined Finite Difference simulations. We use an explicit finite difference scheme as this is widely found in the literature. These comparisons are favourable, though we note a strong dependence on the choice of time-step (but in general the time-steps adopted in the BEM analyses are longer than those required in the FDM analyses). Finally, it will be shown that the smaller the value of α, the smaller must be the value of the corresponding time-step.

2 The Anomalous Diffusion Problem

The governing equation for the anomalous diffusion problem is

$$\frac{\partial^\alpha u}{\partial t^\alpha} - D\left(\frac{\partial^2 u}{\partial x^2} + \frac{\partial^2 u}{\partial y^2}\right) = 0, \qquad 0 < \alpha < 1, \tag{2.1}$$

where D is the diffusion coefficient, assumed to be constant. We aim to solve (2.1) for $u(\mathbf{x}, t)$, where t is time, and point $\mathbf{x} = (x, y)$ lies in domain Ω with a boundary $\Gamma = \Gamma_u \cup \Gamma_q$. The solution is to be found subject to boundary and initial conditions:

$$u(\mathbf{x}, t) = \hat{u}(\mathbf{x}, t), \qquad \mathbf{x} \in \Gamma_u, \tag{2.2}$$

$$D\frac{\partial u}{\partial n} = q(\mathbf{x},t) = \hat{q}(\mathbf{x},t), \qquad \mathbf{x} \in \Gamma_q, \tag{2.3}$$

$$u(\mathbf{x},0) = u_0(\mathbf{x}). \tag{2.4}$$

In equation (2.1), the fractional derivative of α-order in the Caputo sense is given by

$$\frac{\partial_C^\alpha u}{\partial t^\alpha} = \frac{1}{\Gamma(1-\alpha)} \int_0^t \frac{1}{(t-\tau)^\alpha} \frac{\partial u(\tau)}{\partial \tau}\, d\tau. \tag{2.5}$$

where $\Gamma(\cdot)$ is the Gamma function, and is not to be confused with the domain boundary. The solution of equation (2.1) becomes easier if one transforms the fractional time derivative on the left hand side into an integer derivative of order 1. To do so, one can use the Riemann-Liouville (RL) fractional derivative, defined as

$$RL^\alpha(u(t)) = \frac{1}{\Gamma(1-\alpha)} \frac{d}{dt} \int_0^t \frac{u(\tau)}{(t-\tau)^\alpha}\, d\tau. \tag{2.6}$$

Other definitions of fractional derivatives can be found in Ortigueira [2]. Note that, from the definitions given by equations (2.5) and (2.6), the Caputo and Riemann-Liouville derivatives are seen to be integrodifferential operators in which the sequence of integration and differentiation is inverted. When the initial conditions are zero, both definitions coincide.

The Riemann-Liouville operator has the following property:

$$RL^{1-\alpha}\left(\frac{\partial^\alpha u(t)}{\partial t^\alpha}\right) = \frac{\partial u}{\partial t}. \tag{2.7}$$

Applying the operator $RL^{1-\alpha}$ to both sides of equation (2.1), one has

$$\frac{\partial u}{\partial t} = DRL^{1-\alpha}\left(\frac{\partial^2 u}{\partial x^2} + \frac{\partial^2 u}{\partial y^2}\right) = \frac{D}{\Gamma(\alpha)} \frac{d}{dt} \int_0^t \frac{1}{(t-\tau)^{1-\alpha}} \left(\frac{\partial^2 u(\mathbf{x},\tau)}{\partial x^2} + \frac{\partial^2 u(\mathbf{x},\tau)}{\partial y^2}\right) d\tau. \tag{2.8}$$

Equation (2.8) is the equation to be solved by the Boundary Element Method and by the Finite Difference Method.

3 The Boundary Element Method

The boundary integral equation used in the BEM may be obtained from the weighted residual approach, e.g. Brebbia et al. [27], Zienkiewicz and Morgan [28]. The basic steps can be summarised as follows: i) the fundamental solution of the steady-state problem plays the role of the weighting function, w, for the domain residuals; ii) the weighting functions for the residuals at the boundaries Γ_u and Γ_q, denoted here, respectively, as $\overline{w}$ and $\overline{\overline{w}}$, are determined as some functions that conveniently avoid unnecessary approximation of the boundary conditions.

In the absence of a fundamental solution for the PDE under consideration, we propose the use of the steady state fundamental solution in a time-dependent problem. This causes a domain integral to arise, in which the integrand contains the time derivative of the variable of interest, i.e. $\dot{u}$. For this reason, the present formulation can be classified as a D-BEM type formulation.

The weighted residual equation is written as

$$\int_\Omega \left(DRL^{1-\alpha}\left(\frac{\partial^2 u}{\partial x^2} + \frac{\partial^2 u}{\partial y^2}\right) - \frac{\partial u}{\partial t}\right) w\, d\Omega + \int_{\Gamma_u} (u-\hat{u})\, \bar{w}\, d\Gamma + \int_{\Gamma_q} (q-\hat{q})\, \bar{\bar{w}}\, d\Gamma = 0. \tag{3.1}$$

Here, $w = w(\xi, \mathbf{x})$, where $\xi = (\xi_x, \xi_y)$, is the source point and $\mathbf{x} = (x, y)$ is the field point.

After application of the divergence theorem, the domain integral in equation (3.1) can be rewritten as

$$\begin{aligned}\int_\Omega \left(DRL^{1-\alpha}\left(\frac{\partial^2 u}{\partial x^2}+\frac{\partial^2 u}{\partial y^2}\right)-\frac{\partial u}{\partial t}\right) w\, d\Omega \;=\; & \int_\Gamma \left(DRL^{1-\alpha}\left(\frac{\partial u}{\partial x}n_x+\frac{\partial u}{\partial y}n_y\right)\right) w\, d\Gamma - \\ & \int_\Gamma \left(DRL^{1-\alpha}(u)\left(\frac{\partial w}{\partial x}n_x+\frac{\partial w}{\partial y}n_y\right)\right)\, d\Gamma + \\ & \int_\Omega \left(DRL^{1-\alpha}(u)\left(\frac{\partial^2 w}{\partial x^2}+\frac{\partial^2 w}{\partial y^2}\right)\right)\, d\Omega - \int_\Omega \left(\frac{\partial u}{\partial t}\right) w\, d\Omega. \end{aligned} \tag{3.2}$$

From (3.2), q becomes

$$q = D\frac{\partial u}{\partial n} = D\left(\frac{\partial u}{\partial x}n_x+\frac{\partial u}{\partial y}n_y\right), \tag{3.3}$$

and we define a similar quantity, Q, containing the derivative of the weighting function, as

$$Q = D\frac{\partial w}{\partial n} = D\left(\frac{\partial w}{\partial x}n_x+\frac{\partial w}{\partial y}n_y\right), \tag{3.4}$$

where n_x and n_y are the components of the unit outward normal to the boundary.

Recalling that

$$RL^{\alpha-1}(u) = \frac{1}{\Gamma(\alpha)}\frac{d}{dt}\int_0^t \frac{u(\mathbf{x},\tau)}{(t-\tau)^{1-\alpha}}\, d\tau, \tag{3.5}$$

and discretising time t into intervals of duration Δt, one can consider the integral in equation (3.5) time-step by time-step, over each of which we assume u to be constant, i.e.

$$\begin{aligned}\frac{d}{dt}\int_0^t \frac{u(\mathbf{x},\tau)}{(t-\tau)^{1-\alpha}}d\tau\Big|_{t=(n+1)\Delta t} \;=\; & \frac{d}{dt}\int_0^{\Delta t}\frac{1}{(t-\tau)^{1-\alpha}}d\tau u(\mathbf{x},\Delta t)\Big|_{t=(n+1)\Delta t} + \\ & \frac{d}{dt}\int_{\Delta t}^{2\Delta t}\frac{1}{(t-\tau)^{1-\alpha}}d\tau u(\mathbf{x},2\Delta t)\Big|_{t=(n+1)\Delta t} + \\ & \frac{d}{dt}\int_{2\Delta t}^{3\Delta t}\frac{1}{(t-\tau)^{1-\alpha}}d\tau u(\mathbf{x},3\Delta t)\Big|_{t=(n+1)\Delta t} + \cdots + \\ & \frac{d}{dt}\int_{n\Delta t}^{(n+1)\Delta t}\frac{1}{(t-\tau)^{1-\alpha}}d\tau u(\mathbf{x},(n+1)\Delta t)\Big|_{t=(n+1)\Delta t}. \end{aligned} \tag{3.6}$$

Equation (3.6) can be written in a more simplified way:

$$\begin{aligned}\frac{d}{dt}\int_0^t \frac{u(\mathbf{x},\tau)}{(t-\tau)^{1-\alpha}}d\tau\Big|_{t=(n+1)\Delta t} \;=\; & \frac{d}{dt}\int_0^{\Delta t}\frac{1}{(t-\tau)^{1-\alpha}}d\tau u_1\Big|_{t=(n+1)\Delta t} + \\ & \frac{d}{dt}\int_{\Delta t}^{2\Delta t}\frac{1}{(t-\tau)^{1-\alpha}}d\tau u_2\Big|_{t=(n+1)\Delta t} + \\ & \frac{d}{dt}\int_{2\Delta t}^{3\Delta t}\frac{1}{(t-\tau)^{1-\alpha}}d\tau u_3\Big|_{t=(n+1)\Delta t} + \cdots + \\ & \frac{d}{dt}\int_{n\Delta t}^{(n+1)\Delta t}\frac{1}{(t-\tau)^{1-\alpha}}d\tau u_{n+1}\Big|_{t=(n+1)\Delta t}, \end{aligned} \tag{3.7}$$

where $u_k = u(x,t_k) = u(x,k\Delta t)$.

A generic term in the previous equation can be written as

$$\frac{d}{dt}\int_{j\Delta t}^{(j+1)\Delta t}\frac{1}{(t-\tau)^{1-\alpha}}d\tau u_{j+1}\Big|_{t=(n+1)\Delta t} = \Delta t^{\alpha-1}\left[\frac{1}{(n+1-j)^{1-\alpha}}-\frac{1}{(n-j)^{1-\alpha}}\right]u_{j+1}. \tag{3.8}$$

Introducing new notation for the term between brackets as

$$B_{(n+1)(j+1)} := \left[\frac{1}{(n+1-j)^{1-\alpha}} - \frac{1}{(n-j)^{1-\alpha}}\right]. \tag{3.9}$$

one has:

$$RL^{1-\alpha}(u)\Big|_{t=(n+1)\Delta t} = \frac{\Delta t^{\alpha-1}}{\Gamma(\alpha)}\left[u_{n+1} + \sum_{j=0}^{n-1} B_{(n+1)(j+1)} u_{j+1}\right]. \tag{3.10}$$

Note that one can also write

$$RL^{1\alpha}(q)\Big|_{t=(n+1)\Delta t} = \frac{\Delta t^{\alpha-1}}{\Gamma(\alpha)}\left[q_{n+1} + \sum_{j=0}^{n-1} B_{(n+1)(j+1)} q_{j+1}\right]. \tag{3.11}$$

Substitution of equations (3.10) and (3.11) into equation (3.2), and recalling equations (3.3) and (3.4), results in

$$\begin{aligned}\frac{\Delta t^{\alpha-1}}{\Gamma(\alpha)}\int_\Gamma \left[q_{n+1} + \sum_{j=0}^{n-1} B_{(n+1)(j+1)} q_{j+1}\right] w d\Gamma - \frac{\Delta t^{\alpha-1}}{\Gamma(\alpha)}\int_\Gamma \left[u_{n+1} + \sum_{j=0}^{n-1} B_{(n+1)(j+1)} u_{j+1}\right] Q d\Gamma + \\ \frac{\Delta t^{\alpha-1}}{\Gamma(\alpha)}\int_\Omega \left[u_{n+1} + \sum_{j=0}^{n-1} B_{(n+1)(j+1)} u_{j+1}\right] D\left(\frac{\partial^2 w}{\partial x^2} + \frac{\partial^2 w}{\partial y^2}\right) d\Omega - \frac{1}{D}\int_\Omega \dot{u}_{n+1} w d\Omega + \\ \int_{\Gamma_u} u_{n+1}\overline{w} d\Gamma - \int_{\Gamma_u} \hat{u}_{n+1}\overline{w} d\Gamma + \int_{\Gamma_q} q_{n+1}\overline{\overline{w}} d\Gamma - \int_{\Gamma_q} \hat{q}_{n+1}\overline{\overline{w}} d\Gamma = 0.\end{aligned} \tag{3.12}$$

As mentioned before, the weighting functions $\overline{w}$ and $\overline{\overline{w}}$ can be chosen conveniently to avoid approximations to the boundary conditions. This is done simply by taking

$$\overline{w} = \frac{\Delta t^{\alpha-1}}{\Gamma(\alpha)} Q, \tag{3.13}$$

and

$$\overline{\overline{w}} = -\frac{\Delta t^{\alpha-1}}{\Gamma(\alpha)} w, \tag{3.14}$$

The fundamental solution comes from the solution of the equation

$$D\left(\frac{\partial^2 w}{\partial x^2} + \frac{\partial^2 w}{\partial y^2}\right) = -\delta(\mathbf{x} - \xi). \tag{3.15}$$

Then, the first domain integral on the left hand side of equation (3.12) becomes

$$\frac{\Delta t^{\alpha-1}}{\Gamma(\alpha)}\int_\Omega \left[u_{n+1} + \sum_{j=0}^{n-1} B_{(n+1)(j+1)} u_{j+1}\right] D\left(\frac{\partial^2 w}{\partial x^2} + \frac{\partial^2 w}{\partial y^2}\right) d\Omega = -\frac{\Delta t^{\alpha-1}}{\Gamma(\alpha)}\left[u_{n+1}(\xi) + \sum_{j=0}^{n-1} B_{(n+1)(j+1)} u_{j+1}(\xi)\right]. \tag{3.16}$$

Finally, $\dot{u}_{n+1}$ in the second domain integral on the left hand side of equation (3.12) is approximated using a backward finite difference formula (see Smith [29]), i.e.

$$\dot{u}_{n+1} = \frac{u_{n+1} - u_n}{\Delta t}. \tag{3.17}$$

After (3.13), (3.14), (3.16) and (3.17) are substituted into (3.2), the basic BEM integral equation arises. For $\xi \in \Gamma$, it can be written as:

$$c(\xi)u_{n+1}(\xi) = \int_\Gamma q_{n+1} w d\Gamma - \int_\Gamma u_{n+1} Q d\Gamma - \frac{\Gamma(\alpha)}{\Delta t^\alpha} \int_\Omega (u_{n+1} - u_n)\, w d\Omega - \sum_{j=0}^{n-1} B_{(n+1)(j+1)} \left[c(\xi) u_{j+1}(\xi) + \int_\Gamma u_{j+1} Q d\Gamma - \int_\Gamma q_{j+1} w d\Gamma \right], \tag{3.18}$$

where the coefficient $c(\xi)$ is the usual jump term coefficient from the standard BEM formulation. After carrying out boundary and domain discretisation, the resulting system can be written in matrix form as

$$\begin{bmatrix} \mathbf{H}^{bb} & \mathbf{0} \\ \mathbf{H}^{db} & \mathbf{I} \end{bmatrix} \begin{Bmatrix} \mathbf{u}^b_{n+1} \\ \mathbf{u}^d_{n+1} \end{Bmatrix} = \begin{bmatrix} \mathbf{G}^{bb} \\ \mathbf{G}^{db} \end{bmatrix} \left\{ \mathbf{q}^b_{n+1} \right\} - \sum_{j=1}^{n} B_{(n+1)(j+1)} \left(\begin{bmatrix} \mathbf{H}^{bb} & \mathbf{0} \\ \mathbf{H}^{db} & \mathbf{I} \end{bmatrix} \begin{Bmatrix} \mathbf{u}^b_{n+1} \\ \mathbf{u}^d_{n+1} \end{Bmatrix} \right) + \frac{\Gamma(\alpha)}{\Delta t^\alpha} \begin{bmatrix} \mathbf{M}^{bb} & \mathbf{M}^{bd} \\ \mathbf{M}^{db} & \mathbf{M}^{dd} \end{bmatrix} \begin{Bmatrix} \mathbf{u}^b_{n+1} - \mathbf{u}^b_n \\ \mathbf{u}^d_{n+1} - \mathbf{u}^d_n \end{Bmatrix}. \tag{3.19}$$

Here, $\mathbf{I}$ is the identity matrix and the superscripts b and d correspond to boundary and domain variables. Double superscripts are interpreted as the first indicating the position of the source point and the second the position of the field point. The null matrix shows that there is no dependence of the boundary values upon the domain values.

The fundamental solution is given by

$$w = w(\xi, \mathbf{x}) = -\frac{1}{2\pi D} \ln r, \tag{3.20}$$

where r is the distance between the field and source points. The fundamental solution is quite simple, making the BEM formulation attractive and versatile. For example, the development of a BEM formulation for the solution of the wave-diffusion equation, for which $1 < \alpha < 2$, is quite straightforward. This will be the subject of a future article.

For anisotropic media, the governing differential equation (2.1) needs to be restated in terms of D_x and D_y, different diffusion coefficients acting in the different directions. We have

$$\frac{\partial^\alpha u}{\partial t^\alpha} = D_x \frac{\partial^2 u}{\partial x^2} + D_y \frac{\partial^2 u}{\partial y^2}. \tag{3.21}$$

The development of a D-BEM formulation for the solution of (3.21) follows the same steps as those presented above for isotropic media, though the fundamental solution becomes [30, 31]

$$w = w(\xi, \mathbf{x}) = -\frac{1}{2\pi\sqrt{D_x D_y}} \ln \sqrt{(x - \xi_x)^2 + \frac{D_x}{D_y}(y - \xi_x)^2}. \tag{3.22}$$

The fundamental solution (3.20) for an isotropic medium can be looked upon as a particular case that for an anisotropic medium, given by equation (3.22).

3.1 Finite Difference Method

In the absence of a known analytical solution for some of the examples presented here, and in order to validate the BEM results, a Finite Difference Method formulation was also developed. It is presented

briefly in what follows, always bearing in mind that the main purpose of the article is the development of a BEM formulation.

The application of the forward finite difference formula to equation (2.6) enables one to write

$$\frac{\partial u}{\partial t} = \frac{D}{\Gamma(\alpha)} \frac{1}{\Delta t} \left(\int_0^{t+\Delta t} \frac{u_{xx}(\mathbf{x},\tau) + u_{yy}(\mathbf{x},\tau)}{(t+\Delta t-\tau)^{1-\alpha}}\, d\tau - \int_0^{t} \frac{u_{xx}(\mathbf{x},\tau) + u_{yy}(\mathbf{x},\tau)}{(t-\tau)^{1-\alpha}}\, d\tau \right), \tag{3.23}$$

where

$$u_{xx} = \frac{\partial^2 u}{\partial x^2}, \qquad u_{yy} = \frac{\partial^2 u}{\partial y^2}.$$

If, in equation (3.23), $t = t_n = n\Delta t$, where $n = 0, 1, \ldots$, the first integral on the right hand side of equation (3.23) can be evaluated numerically by the backward rectangular rule, thus generating the expression

$$\int_0^{n\Delta t+\Delta t} \frac{u_{xx}(\mathbf{x},\tau) + u_{yy}(\mathbf{x},\tau)}{(t+\Delta t-\tau)^{1-\alpha}}\, d\tau = \sum_{k=0}^{n} \frac{u_{xx}(\mathbf{x},k\Delta t) + u_{yy}(\mathbf{x},k\Delta t)}{(n+1-k)^{1-\alpha}} \Delta t^{\alpha}. \tag{3.24}$$

For the evaluation of the second integral on the right hand side of equation (3.23), the expression is

$$\int_0^{n\Delta t} \frac{u_{xx}(\mathbf{x},\tau) + u_{yy}(\mathbf{x},\tau)}{(t-\tau)^{1-\alpha}}\, d\tau = \sum_{k=0}^{n-1} \frac{u_{xx}(\mathbf{x},k\Delta t) + u_{yy}(\mathbf{x},k\Delta t)}{(n-k)^{1-\alpha}} \Delta t^{\alpha}. \tag{3.25}$$

Substitution of (3.24) and (3.25) into (3.23) yields the expression

$$\frac{\partial u}{\partial t} = \frac{D}{\Gamma(\alpha)} \Delta t^{\alpha-1} \left(\sum_{k=0}^{n} \frac{u_{xx}(\mathbf{x},k\Delta t) + u_{yy}(\mathbf{x},k\Delta t)}{(n+1-k)^{1-\alpha}} \Delta t^{\alpha} - \sum_{k=0}^{n-1} \frac{u_{xx}(\mathbf{x},k\Delta t) + u_{yy}(\mathbf{x},k\Delta t)}{(n-k)^{1-\alpha}} \Delta t^{\alpha} \right), \tag{3.26}$$

Equation (3.2) can be rearranged as follows

$$\begin{aligned} \frac{\partial u}{\partial t} &= \frac{D}{\Gamma(\alpha)} \Delta t^{\alpha-1} \left(u_{xx}(\mathbf{x},n\Delta t) + u_{yy}(\mathbf{x},n\Delta t) \right) + \\ & \frac{D}{\Gamma(\alpha)} \sum_{k=0}^{n-1} \left(\frac{1}{(n+1-k)^{1-\alpha}} - \frac{1}{(n-k)^{1-\alpha}} \right) \left(u_{xx}(\mathbf{x},k\Delta t) + u_{yy}(\mathbf{x},k\Delta t) \right). \end{aligned} \tag{3.27}$$

This can be written in a simplified form, as

$$\frac{\partial u}{\partial t} = \frac{D}{\Gamma(\alpha)} \Delta t^{\alpha-1} \left(u_{xx}^{n} + u_{yy}^{n} + \sum_{k=0}^{n-1} B_{nk} \left(u_{xx}^{k} + u_{yy}^{k} \right) \right), \tag{3.28}$$

where

$$\begin{aligned} u_{xx}^{j} &= u_{xx}(\mathbf{x}, j\Delta t), \qquad u_{yy}^{j} = u_{yy}(\mathbf{x}, j\Delta t), \\ B_{nk} &= \frac{1}{(n+1-k)^{1-\alpha}} - \frac{1}{(n-k)^{1-\alpha}}. \end{aligned} \tag{3.29}$$

Note that the factor B_{nk}, defined in equation (3.29), is equivalent to the one already defined in the BEM formulation, see equation (3.9). The difference in the index appears because the FDM formulation, as developed here, is explicit, whereas the BEM formulation is implicit.

The first order time derivative on the left hand side of equation (3.23), computed at $t = t_n$, and the second order spatial derivatives with respect to x and y in equation (3.28) computed, respectively, at $x = x_i$ and at $y = y_j$, may be substituted into their finite difference formulae (Smith [29]), giving

$$\frac{\partial u}{\partial t} = \frac{u_{i,j}^{n+1} - u_{i,j}^{n}}{\Delta t}, \quad u_{xx} = \frac{u_{i+1,j}^{n} - 2u_{i,j}^{n} + u_{i-1,j}^{n}}{\Delta x^2}, \quad u_{yy} = \frac{u_{i,j+1}^{n} - 2u_{i,j}^{n} + u_{i,j-1}^{n}}{\Delta y^2}.$$

Finally, the FDM equation that corresponds to the equation (2.1) can be written as

$$u_{i,j}^{n+1} = u_{i,j}^{n} + \frac{D}{\Gamma(\alpha)}\frac{\Delta t^{\alpha}}{\Delta x^2}\left(u_{i+1,j}^{n} - 2u_{i,j}^{n} + u_{i-1,j}^{n} + \sum_{k=0}^{n-1} B_{nk}\left(u_{i+1,j}^{k} - 2u_{i,j}^{k} + u_{i-1,j}^{k}\right)\right) + \frac{D}{\Gamma(\alpha)}\frac{\Delta t^{\alpha}}{\Delta y^2}\left(u_{i,j+1}^{n} - 2u_{i,j}^{n} + u_{i,j-1}^{n} + \sum_{k=0}^{n-1} B_{nk}\left(u_{i,j+1}^{k} - 2u_{i,j}^{k} + u_{i,j-1}^{k}\right)\right). \tag{3.30}$$

Equation (3.30) is valid for $n > 0$. When $n = 0$, it becomes

$$u_{i,j}^{1} = u_{i,j}^{0} + \frac{D}{\Gamma(\alpha)}\frac{\Delta t^{\alpha}}{\Delta x^2}\left(u_{i+1,j}^{0} - 2u_{i,j}^{0} + u_{i-1,j}^{0}\right) + \frac{D}{\Gamma(\alpha)}\frac{\Delta t^{\alpha}}{\Delta y^2}\left(u_{i,j+1}^{0} - 2u_{i,j}^{0} + u_{i,j-1}^{0}\right). \tag{3.31}$$

Naturally, anisotropic problems can be dealt with by simply substituting the diffusion coefficients, D_x and D_y, in the second and third terms on the right hand side of equations (3.30) and (3.31), for D.

Note that equation (3.30) corresponds to an explicit forward time centred space (FTCS) scheme with the direct integration of the Riemann-Liouville derivative. The same approach is followed by Yuste and Acedo [29], but with the Grunwald-Letnikov discretisation of the Riemann-Liouville derivative.

4 Examples

A series of test examples are presented in this section to demonstrate the numerical performance of the new BEM algorithm. The results are presented as functions of time for a selected domain point and as functions of the spatial coordinates for chosen values of time. For $\alpha = 1.0$, in all examples, the BEM results are compared with the corresponding analytical solution. The time-step in the BEM and FDM analyses will be referred to, respectively, as Δt_{BEM} and Δt_{FDM}. The examples are presented without units; any consistent set may be used.

4.1 Domain under initial condition

In the first example we consider a rectangular domain defined in the region $0 \leq x \leq \pi$ and $0 \leq y \leq \frac{\pi}{2}$. The boundary conditions are

$$u(0, y, t) = u(\pi, y, t) = 0 \tag{4.1}$$

and the initial condition is

$$u(x, y, 0) = u_0(x, y) = \sin x \tag{4.2}$$

so that this is a 1D problem. To simulate this problem through a 2D formulation, the following boundary conditions are adopted at $y = 0$ and $y = \frac{\pi}{2}$:

$$q(x, 0, t) = q\left(x, \frac{\pi}{2}, t\right) = 0. \tag{4.3}$$

The analytical solution for fractional values of α, taken from Murilo and Yuste [8] and Ray [32], is

$$u(x, y, t) = E_{\alpha}\left(-t^{\alpha}\right)\sin x. \tag{4.4}$$

in which E_{α} is the Mittag-Leffler function (see Haubold et al. [33]) and is defined as

$$E_{\alpha}(z) = \sum_{k=0}^{\infty} \frac{z^k}{\Gamma(1 + \alpha k)}, \tag{4.5}$$

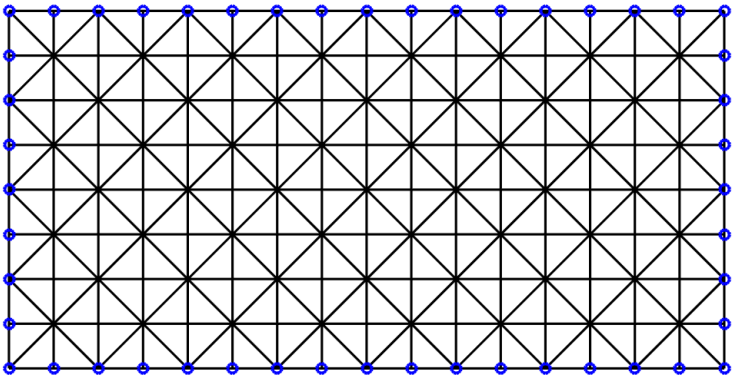

Figure 4.1: BEM mesh for examples 1, 2 and 3.

where $z \in \mathbb{C}$. For the case $\alpha = 1$, one has

$$E_1(z) = e^z, \tag{4.6}$$

and equation (4.4) becomes the well-known analytical solution of the diffusion problem; this means that the analytical solution for the diffusion equation can be looked upon as a particular case of that for anomalous diffusion. We use the following notation in this paper to describe the BEM meshes: n_Γ represents the number of linear boundary elements, and n_Ω represents the number of triangular linear cells. The BEM mesh depicted in Figure 4.1, is of size $n_\Gamma = 48$ and $n_\Omega = 256$. The analyses were carried out with $D = 1.0$, for $\alpha = 1.0$, 0.8 and 0.5. The results for $u(\pi/2, \pi/4, t)$, $0 \leq t \leq 2$ are depicted in Figure 4.2, whereas the results for $u(x, \pi/4, 0.25)$ and $u(x, \pi/4, 1.0)$, $0 \leq x \leq \pi$ are depicted, respectively, in Figures 4.3 and 4.4. The required time-step duration, found through numerical tests, shows a strong dependence on the parameter α, with smaller values of α requiring smaller time step Δt. In this example, for $\alpha = 1.0$ and $\alpha = 0.8$, $\Delta t_{BEM} = 0.005$, whereas for $\alpha = 0.5$, a shorter time step $\Delta t_{BEM} = 0.0025$ was required.

The results presented in Figures 4.2, 4.3 and 4.4 show good agreement with the analytical solution for this simple first problem.

4.2 Domain with Dirichlet boundary conditions

In the second example, a rectangular domain is defined on the region $0 \leq x \leq 2$ and $0 \leq y \leq 1$.

A zero initial condition, $u(x, y, 0) = 0$, is assumed and we prescribe the boundary conditions

$$u(0, y, t) = 10, \qquad u(2, y, t) = 0, \qquad q(x, 0, t) = q(x, 1, t) = 0. \tag{4.7}$$

This problem can be interpreted as one of heat transfer from the material at $x = 0$ to $x = 2$.

The analyses were carried out with the same mesh as in the previous example, scaled to accommodate the different domain size. The BEM results are compared with those obtained by FDM analyses, carried out with the 1D version of equation (3.31). For $D = 1.0$, the analyses were carried out with $\alpha = 1.0$, 0.8, 0.5, and 0.2.

The results at the mid-point, i.e. $u(1, 0.5, t)$, for times $0 \leq t \leq 4$, are presented in Figure 4.5. The results at $t = 0.25$ and at $t = 1.0$ are shown, respectively, in Figures 4.6 and 4.7. The FDM analyses were carried out with $\Delta x = 0.25$. This value proved to be the best choice in order to obtain stable results, mainly when $\alpha = 0.2$.

For $\alpha = 0.2$, we take $\Delta t_{BEM} = 0.0001$, while for the other values of α the analyses were carried out with $\Delta t_{BEM} = 0.005$. For the FDM analyses, for $\alpha = 0.2$, $\Delta t_{FDM} = 0.00001$, a very small value compared with $\Delta t_{FDM} = 0.001$ for $\alpha = 1.0$, 0.8, 0.5.

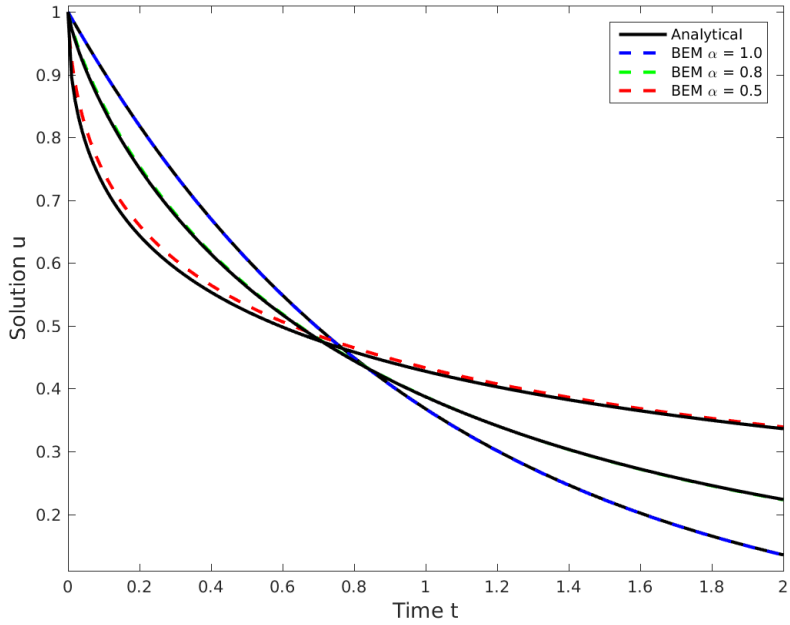

Figure 4.2: Domain under initial condition: results for $u(\pi/2, \pi/4, t)$.

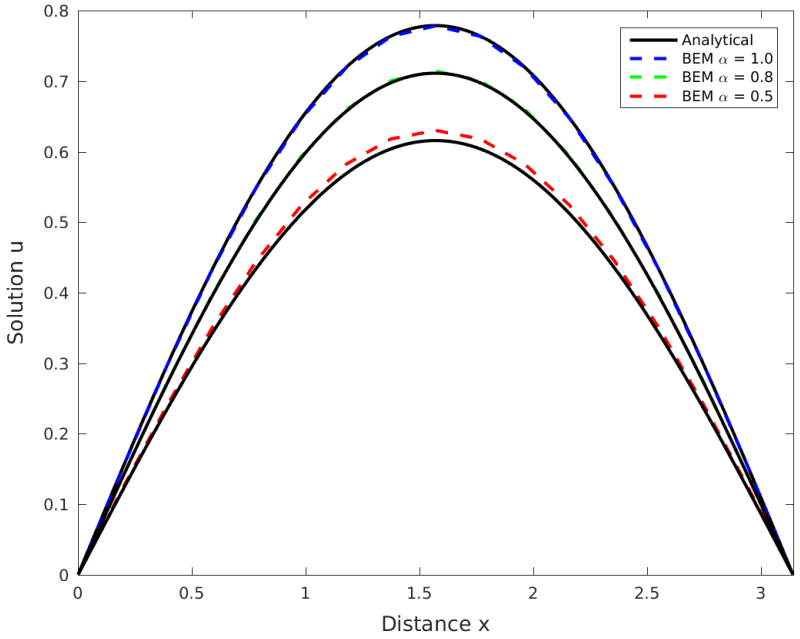

Figure 4.3: Domain under initial condition: results for $u(x, \pi/4, 0.25)$.

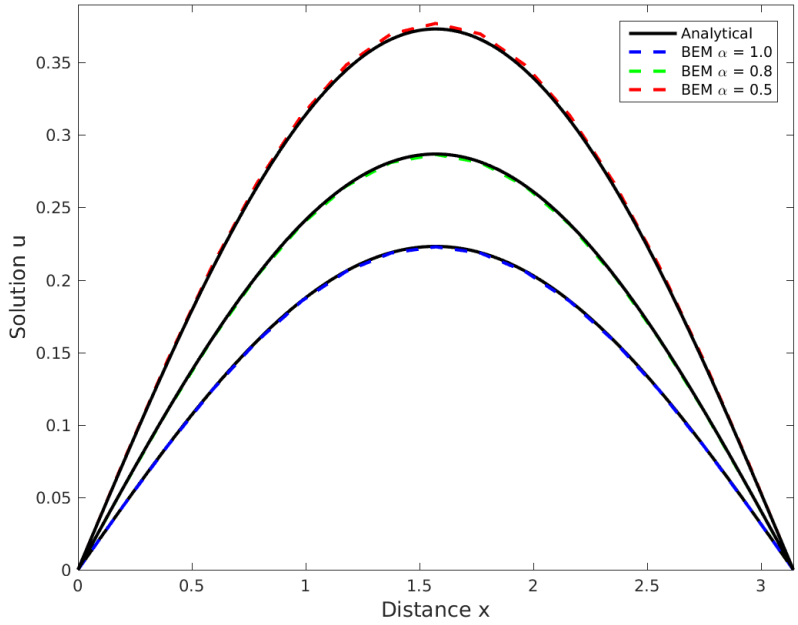

Figure 4.4: Domain under initial condition: results for $u(x, \pi/4, 1.0)$.

Table 4.1: Time steps, Δt suggested by equation (4.8) for FDM grid size $\Delta x = 0.25$.

α	Δt
1.0	3.125×10^{-2}
0.8	1.105×10^{-2}
0.5	4.883×10^{-4}
0.2	1.863×10^{-9}

Yuste and Acedo [15] provide a stability criterion,

$$\frac{D\Delta t^{\alpha}}{\Delta x^2} \leq \frac{1}{2^{2-\alpha}} \tag{4.8}$$

and the values suggested by this formula for $\Delta x = 0.25$ are shown in Table 4.1.

For $\alpha = 0.5$ and $\alpha = 0.2$ the values computed according to equation (4.8) are more conservative than those used in the FDM analyses. However, the same criterion is more flexible for $\alpha = 1.0$ and $\alpha = 0.8$. For the BEM, the development of a stability criterion is an open subject for further research.

As is evident from Figures 4.5-4.7, good agreement is observed between BEM and FDM results for this problem, though again we see some discrepancy between the BEM and FDM in capturing the extreme temporal gradients in the solution for small α in the initial time steps.

4.3 Domain with oscillatory Dirichlet boundary condition

In this section, the same domain and mesh as those in the previous example are considered, under a zero initial condition and subject to the following boundary conditions:

$$u(0, y, t) = 0, \qquad u(2, y, t) = 1 - \cos 2\pi t, \qquad q(x, 0, t) = q(x, 1, t) = 0. \tag{4.9}$$

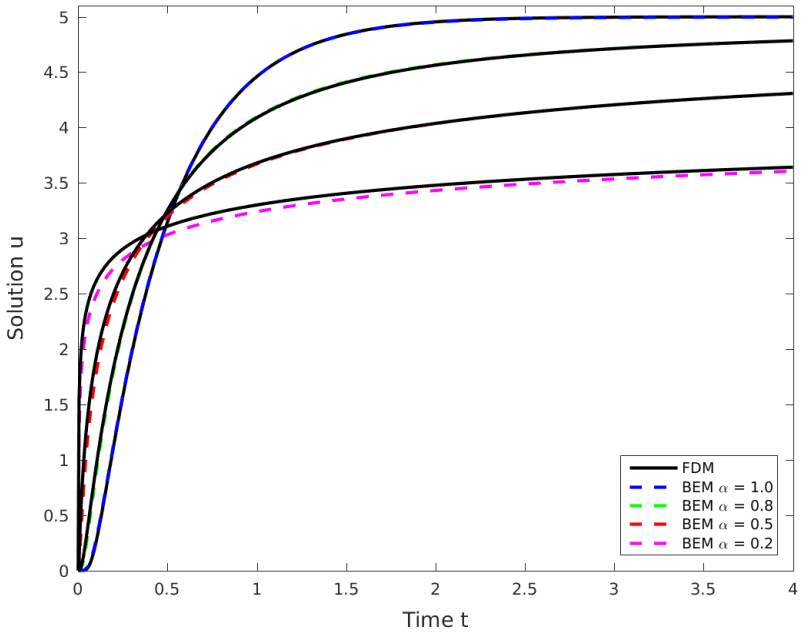

Figure 4.5: Domain with Dirichlet boundary conditions: results for $u(1, 0.5, t)$.

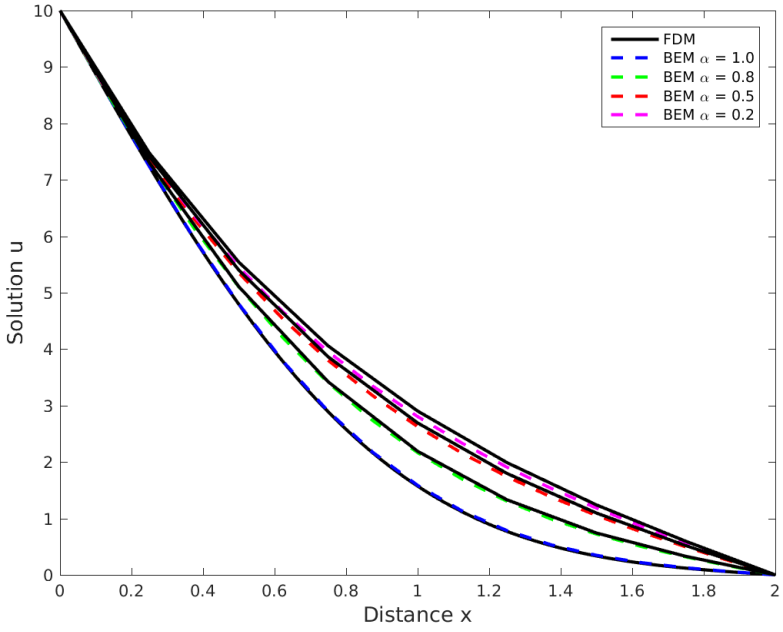

Figure 4.6: Domain with Dirichlet boundary conditions: results for $u(x, 0.5, 0.25)$.

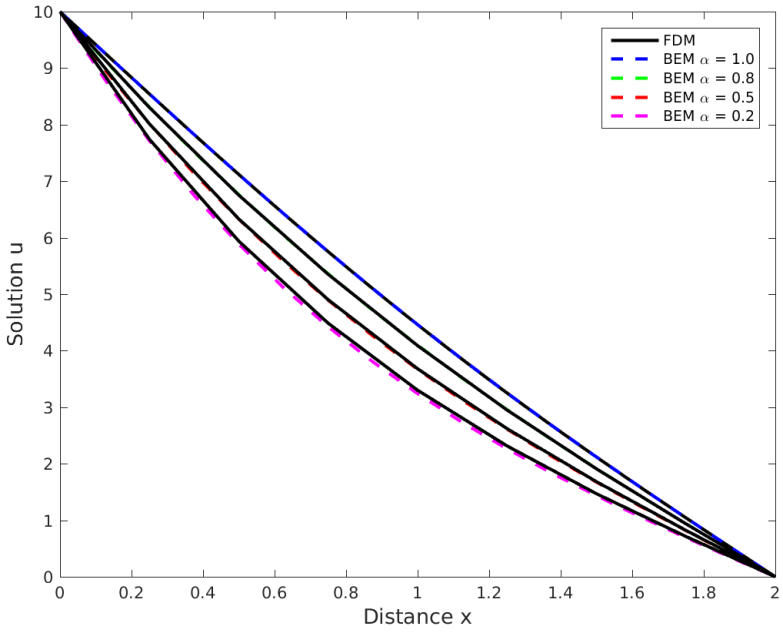

Figure 4.7: Domain with Dirichlet boundary conditions: results for $u(x, 0.5, 1.0)$.

Table 4.2: Time steps used for the example in section 4.3

α	Δt_{BEM}	Δt_{FDM}
1.0	0.0125	0.001
0.8	0.0125	0.001
0.5	0.00315	0.000125

This is a very interesting diffusion example, with an oscillatory solution resulting from the oscillatory boundary condition. Ochiai et al. [34], and Carrer et al. [35] also analysed this problem, with the latter also providing the analytical solution for the case $\alpha = 1.0$.

In this example, a finite difference grid size $\Delta x = 0.0125$ was used, more refined than that used the previous example.

The results for $u(1, 0.5, t)$, $0 \leq t \leq 4$, are presented in Figure 4.8, and the results at $t = 0.25$, $t = 1.0$, and $t = 1.75$ are shown, respectively, in Figures 4.9, 4.10 and 4.11. For the analyses carried out with $D = 1, 0$ and $\alpha = 1.0, 0.8, 0.5$, the BEM and FDM time-step sizes are shown in Table 4.2.

As in the previous examples, BEM analyses enable the use of larger time steps Δt. This is as expected, since the BEM formulation as developed in this work is an implicit scheme, whereas the FDM formulation is explicit and therefore subject to stability constraints on the time step.

The BEM results for $\alpha = 0.5$, presented in Figure 4.10, do not show good agreement with the FDM results. Even with the adoption of a smaller time-step, little change was observed. In spite of this exception, the other results can be considered acceptable and in good agreement with those produced by the FDM.

4.4 Square Domain with Linear Initial Condition

The fourth example is presented to demonstrate the ability of the proposed scheme to handle problems involving anisotropic media. We consider a square domain lying in the region $0 \leq x, y \leq L$. In a smaller,

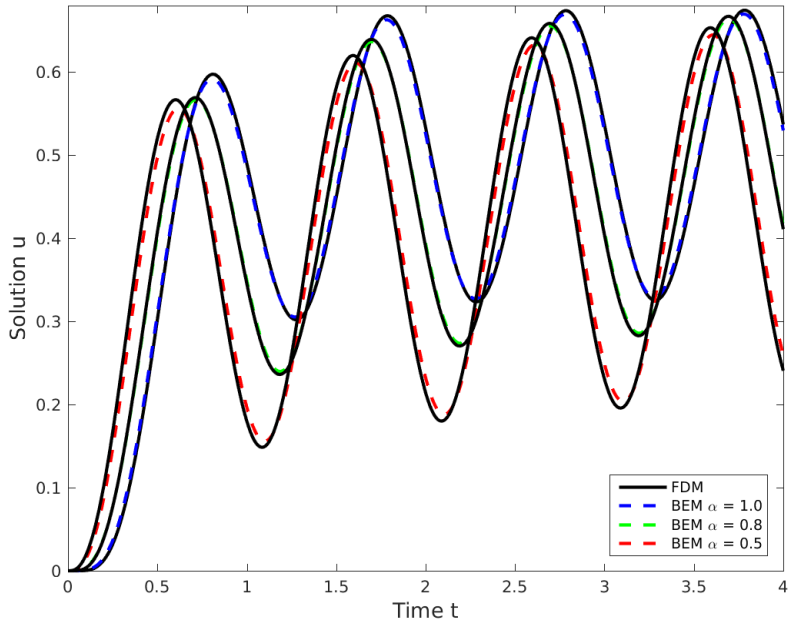

Figure 4.8: Domain with oscillatory Dirichlet boundary condition: results for $u(1, 0.5, t)$.

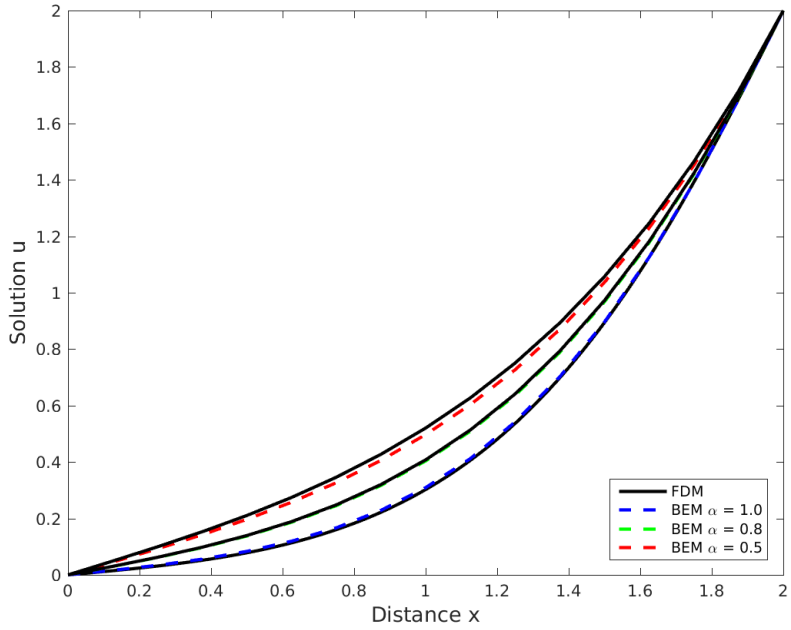

Figure 4.9: Domain with oscillatory Dirichlet boundary condition: results for $u(x, 0.5, 0.25)$.

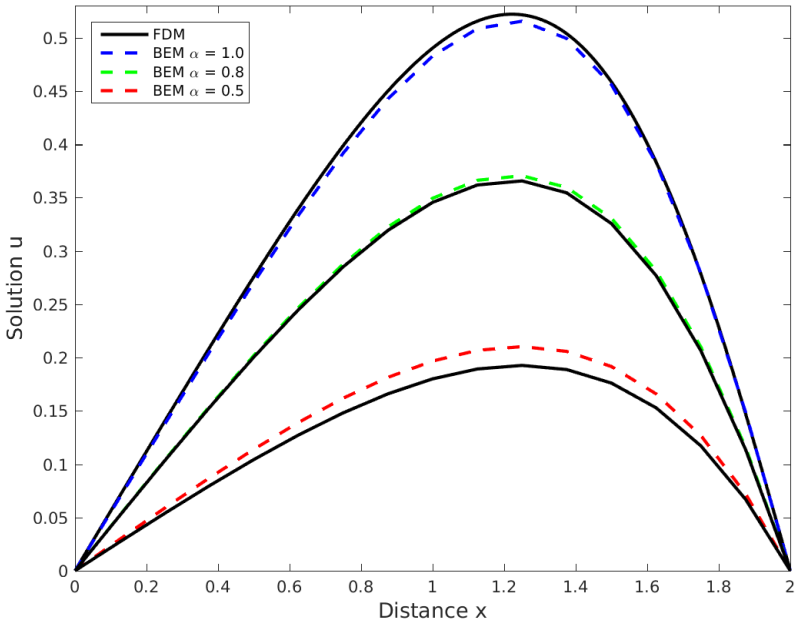

Figure 4.10: Domain with oscillatory Dirichlet boundary condition: results for $u(x, 0.5, 1.0)$.

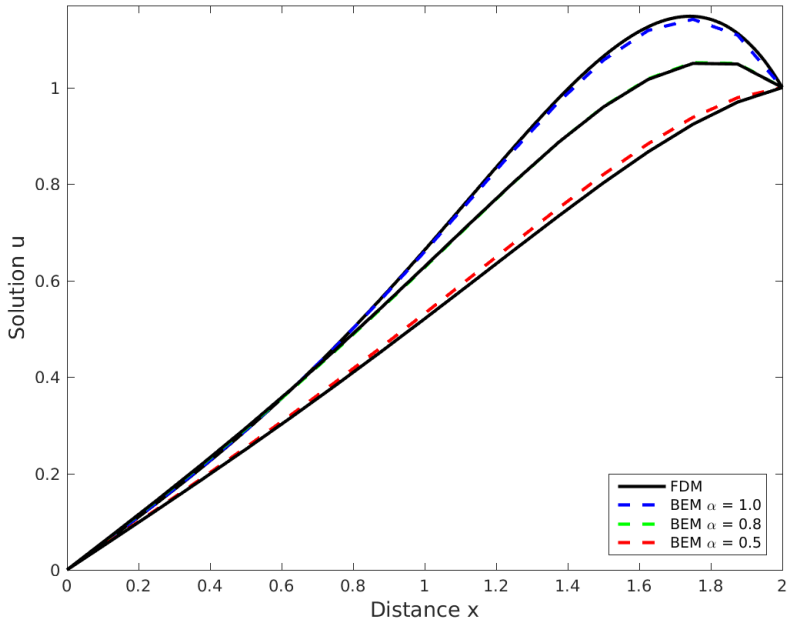

Figure 4.11: Domain with oscillatory Dirichlet boundary condition: results for $u(x, 0.5, 1.75)$.

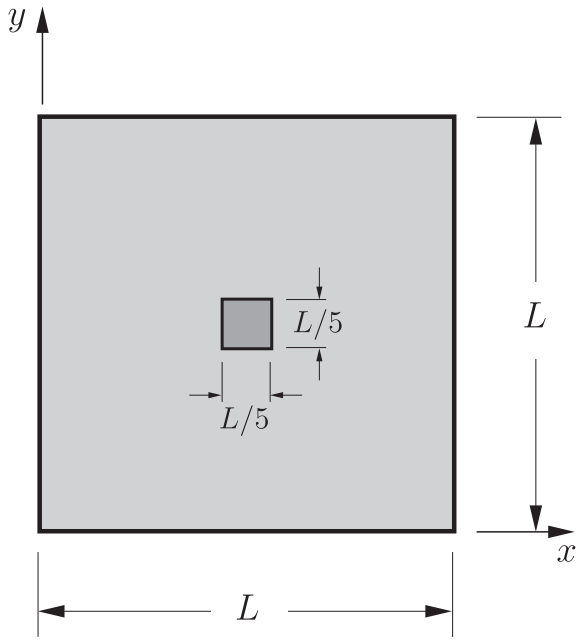

Figure 4.12: Square Domain with Initial Condition: description of the problem.

square sub-domain Ω_0, defined by $2L/5 \leq x, y \leq 3L/5$, as shown in Figure 4.12, an initial condition varies linearly from $u = C_0$ in the centre of Ω_0 to zero on its borders. We take the values $L = 10$ and $C_0 = 10$, and prescribe the boundary conditions to be

$$u(0, y, t) = u(L, y, t) = u(x, 0, t) = u(x, L, t) = 0. \tag{4.10}$$

This problem can also be interpreted as one of heat transfer from a small region inside the domain to the remaining domain, which has a temperature of zero at its outer boundary.

Two cases are considered. In the first case, the medium is assumed to be isotropic with $D = 1.0$. The second case considers an anisotropic medium, with $D_x = 1.0$ and $D_y = 0.1$. We consider $\alpha = 1.0$, 0.8 and 0.5 for both isotropic and anisotropic cases.

The BEM analyses were carried out with three meshes, designated simply as mesh 1, with $n_\Gamma = 40$ and $n_\Omega = 200$, mesh 2, with $n_\Gamma = 80$ and $n_\Omega = 800$, and mesh 3, depicted in Figure 4.13, with $n_\Gamma = 160$ and $n_\Omega = 3200$. For $\alpha \neq 1$, the BEM results are compared with those from FDM analyses, which were carried out by employing three meshes, in each of which the points were at the same positions as those in the corresponding BEM meshes. Consequently, for mesh 1, we have $\Delta x = \Delta y = L/10$, for mesh 2, $\Delta x = \Delta y = L/20$, and finally, for mesh 3, $\Delta x = \Delta y = L/40$. For $\alpha = 1.0$, the convergence of the numerical results to the analytical, or reference, solution is studied through the computation of the relative L^2 error norm, E_2, as follows:

$$E_2 = \frac{||u_{ref} - u_{num}||_{L^2(\Omega)}}{||u_{ref}||_{L^2(\Omega)}} \tag{4.11}$$

where u_{num} represents either the BEM or the FDM results and u_{ref} represents the analytical (or some other) reference solution. For $\alpha \neq 1$, the reference solution comes from FDM analyses carried out with a more refined mesh, that can be called mesh 4, in which $\Delta x = \Delta y = L/80$.

Based on the work by Yuste and Acedo [15], the authors developed an expression for the critical time step for 2D problems, as

$$\Delta t^\alpha \leq \frac{\Delta x^2 \Delta y^2}{2^{2-\alpha}(D_x \Delta y^2 + D_y \Delta x^2)} \tag{4.12}$$

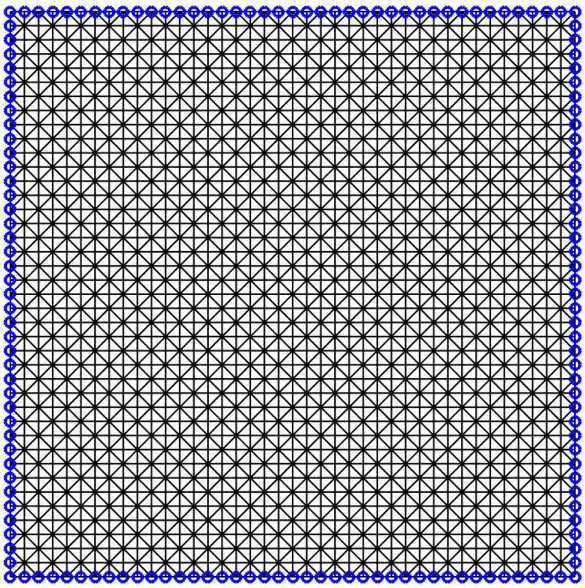

Figure 4.13: Square Domain with Initial Condition: BEM mesh.

Table 4.3: Critical time steps for the 2D problem (isotropic media)

α	Δt_{mesh1}	Δt_{mesh2}	Δt_{mesh3}	Δt_{mesh4}
1.0	2.500×10^{-1}	6.250×10^{-2}	1.563×10^{-2}	N/A
0.8	1.487×10^{-1}	2.628×10^{-2}	4.650×10^{-3}	8.212×10^{-4}
0.5	3.125×10^{-2}	1.953×10^{-3}	1.221×10^{-4}	7.630×10^{-6}

For the regular meshes adopted in this example, this becomes

$$\Delta t^{\alpha} \leq \frac{\Delta L^2}{2^{3-\alpha} D}, \quad \text{for isotropic media} \tag{4.13}$$

$$\Delta t^{\alpha} \leq \frac{\Delta L^2}{2^{2-\alpha}(D_x + D_y)}, \quad \text{for anisotropic media} \tag{4.14}$$

where $\Delta x = \Delta y = \Delta L$. Table 4.3 presents the critical time steps obtained from (4.13) for isotropic media. Very small time steps are seen to be required, and we note also that for small α the number of time steps necessary to reach even moderate times can become prohibitively large.

In all the analyses presented, the same time step was chosen regardless of the medium being isotropic or anisotropic, although from expression (4.12) one can notice that for the anisotropic medium larger time steps could be used.

For $\alpha = 1.0$, BEM and FDM analyses employed the same time step, equal to half the values in the first line of Table 4.3. Figures 4.14 and 4.15 present, respectively, the results for the L^2 error norm, E_2, at $t = 1.0$ for the cases of an isotropic and an anisotropic medium. For $\alpha = 0.8$, the adopted time steps are displayed in Table 4.4 and the convergence comparison between BEM and FDM, in terms of E_2, is shown in Figures 4.16 and 4.17 for isotropic and anisotropic materials respectively. For the reference solution, we take

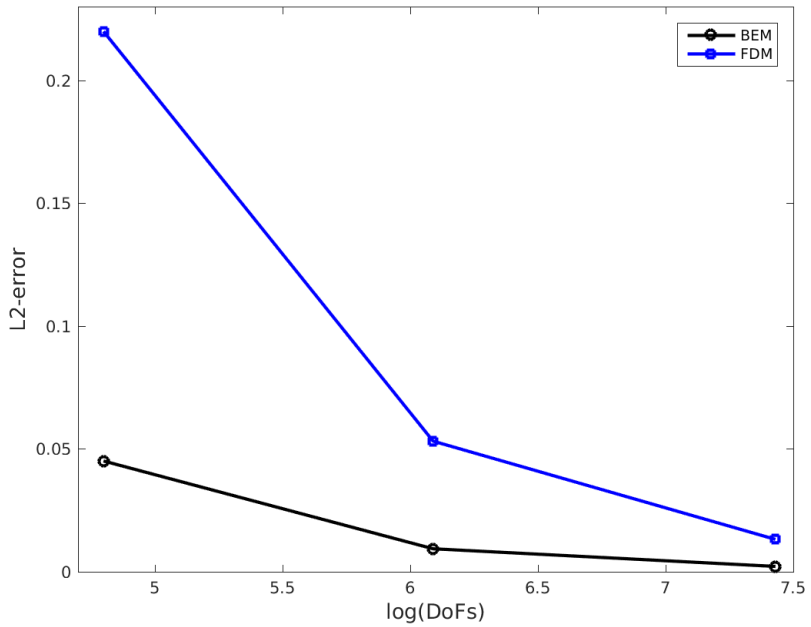

Figure 4.14: Square domain: BEM and FDM convergence for $\alpha = 1.0$ with isotropic medium.

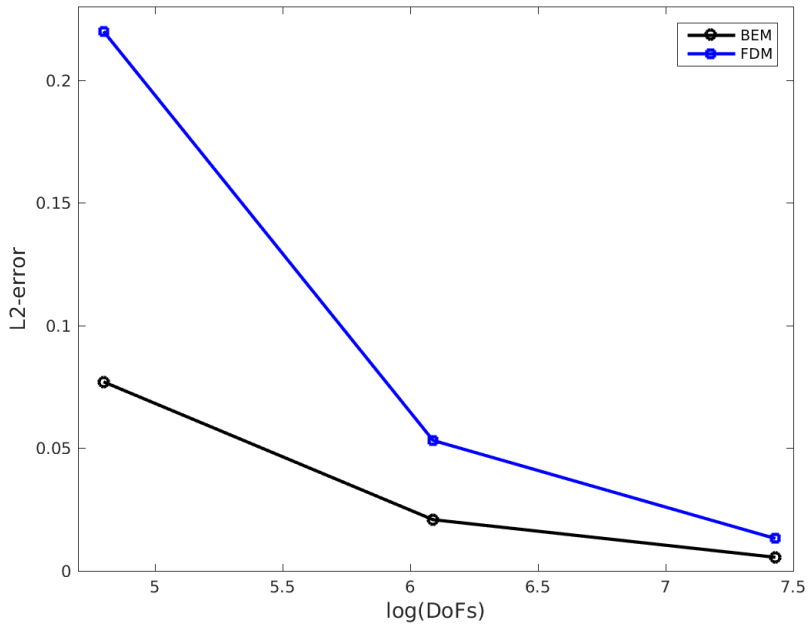

Figure 4.15: Square domain: BEM and FDM convergence for $\alpha = 1.0$ with anisotropic medium.

Table 4.4: Time steps for the 2D problem

	Δt_{BEM}	Δt_{FDM}
mesh 1	0.05	0.05
mesh 2	0.025	0.01
mesh 3	0.0125	0.001

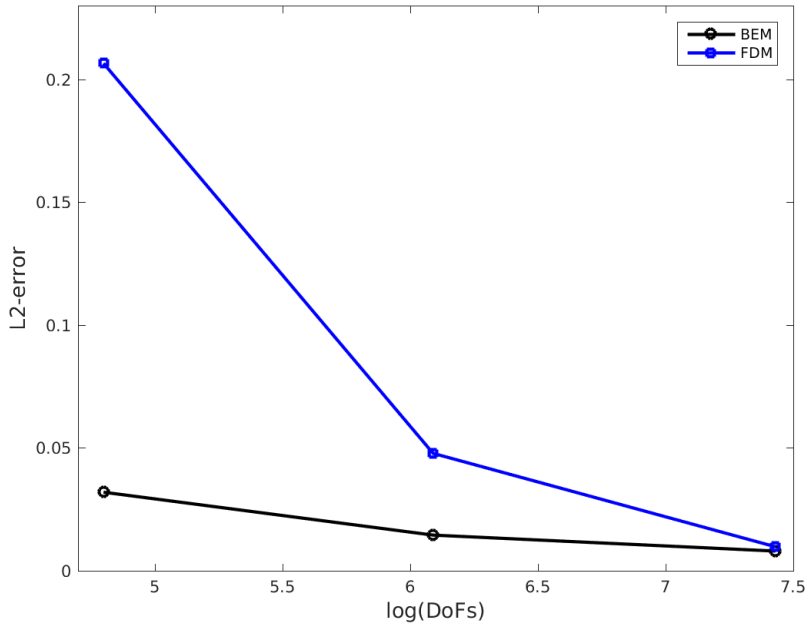

Figure 4.16: Square domain: BEM and FDM convergence for $\alpha = 0.8$ with isotropic medium.

$\Delta t = 5 \times 10^{-4}$. The results shown in Figures 4.14 to 4.17 show the proposed BEM scheme to outperform (considerably) the finite difference method. It is particularly interesting that in this problem the diffusion is driven by conditions within the material and remote from the domain boundary, and this BEM formulation remains very capable of delivering accurate solutions even using the steady-state fundamental solution.

For $\alpha = 0.5$, the computation of the error norm E_2 was made infeasible due to the requirement of a very small time step to obtain the reference results. For this reason, the results corresponding to the FDM for $\alpha = 0.5$ were obtained with the use of mesh 3 and $\Delta t = 1.0 \times 10^{-4}$, in accordance with Table 4.3.

The BEM results obtained with mesh 3 are presented in Figures 4.18, 4.19 and 4.20, respectively, for $\alpha = 1.0, 0.8, 0.5$. As the analytical ($\alpha = 1$) and the FDM ($\alpha = 0.5, 0.8$) results are both visually almost indistinguishable from the BEM results, only the BEM results are shown.

The results at the central point $(L/2, L/2)$ for the first and the second cases are presented, respectively, in Figures 4.21 and 4.22.

4.5 Dirichlet problem on a circular domain

For our final example, we consider a circular domain to demonstrate the BEM performance for a problem that would present difficulties using the FDM. Due to the geometry of the problem, it is conveniently

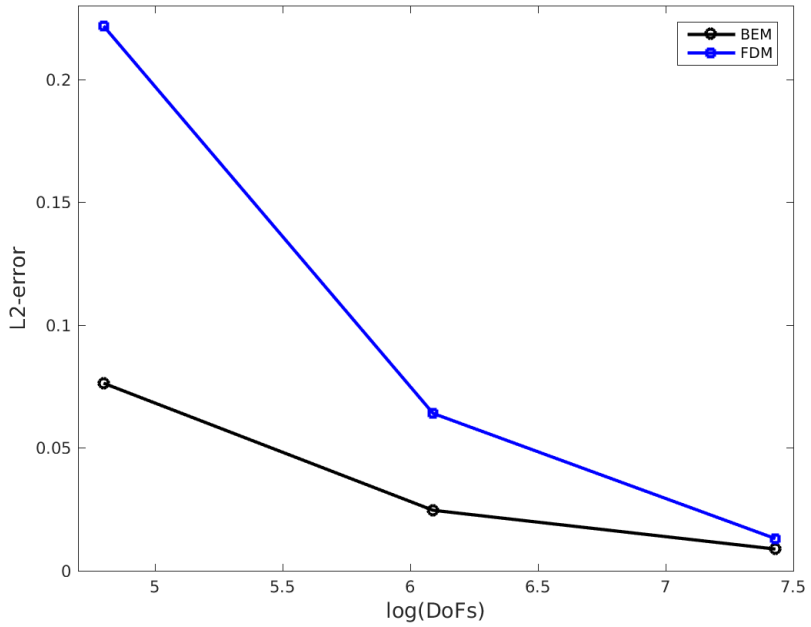

Figure 4.17: Square domain: BEM and FDM convergence for $\alpha = 0.8$ with anisotropic medium.

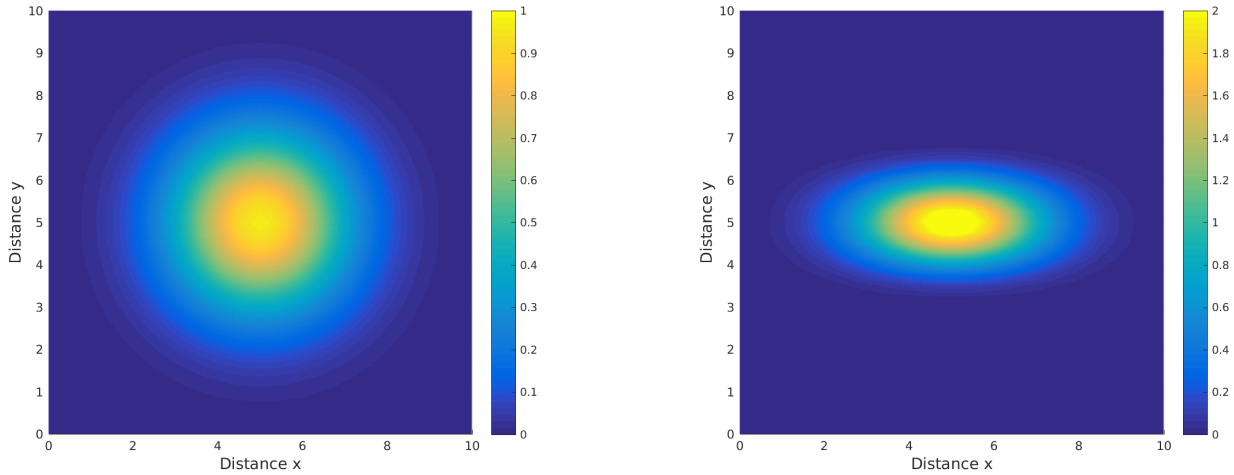

Figure 4.18: BEM results $u(x, y, 1)$ for $\alpha = 1.0$: isotropic medium (left) and anisotropic medium (right).

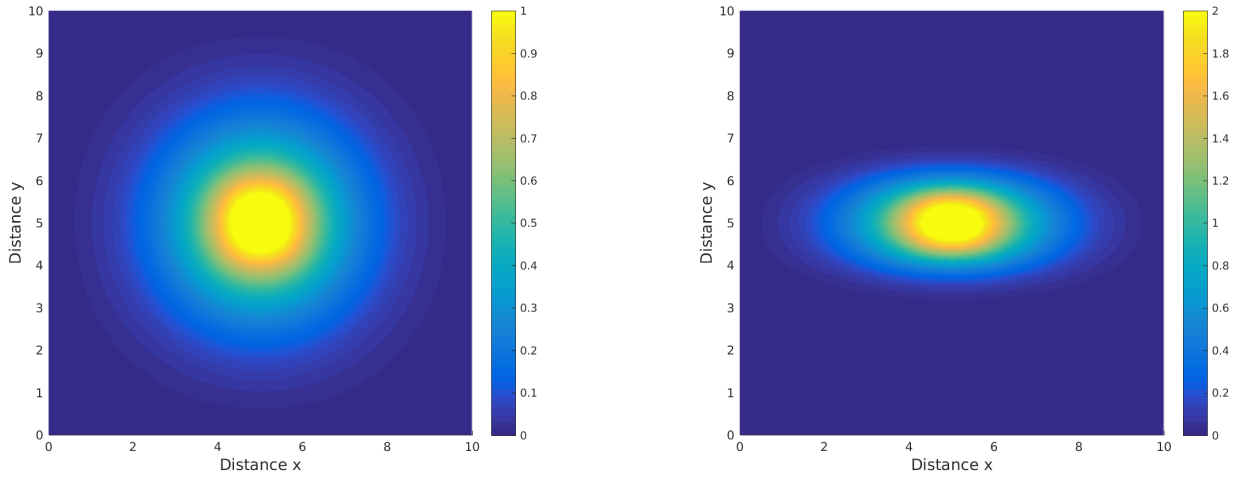

Figure 4.19: BEM results $u(x, y, 1)$ for $\alpha = 0.8$: isotropic medium (left) and anisotropic medium (right).

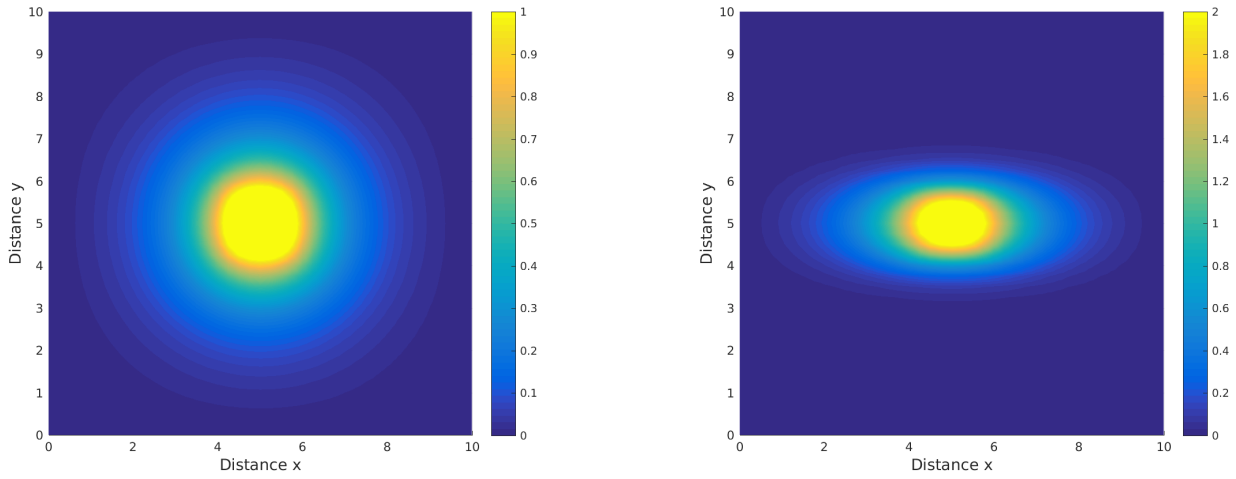

Figure 4.20: BEM results $u(x, y, 1)$ for $\alpha = 0.5$: isotropic medium (left) and anisotropic medium (right).

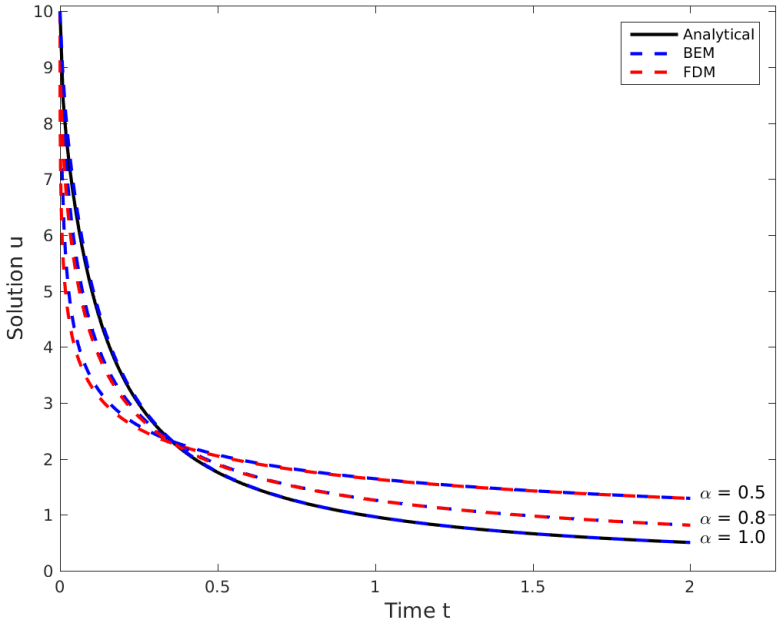

Figure 4.21: Square domain: results $u(L/2, L/2, t)$ for the isotropic medium.

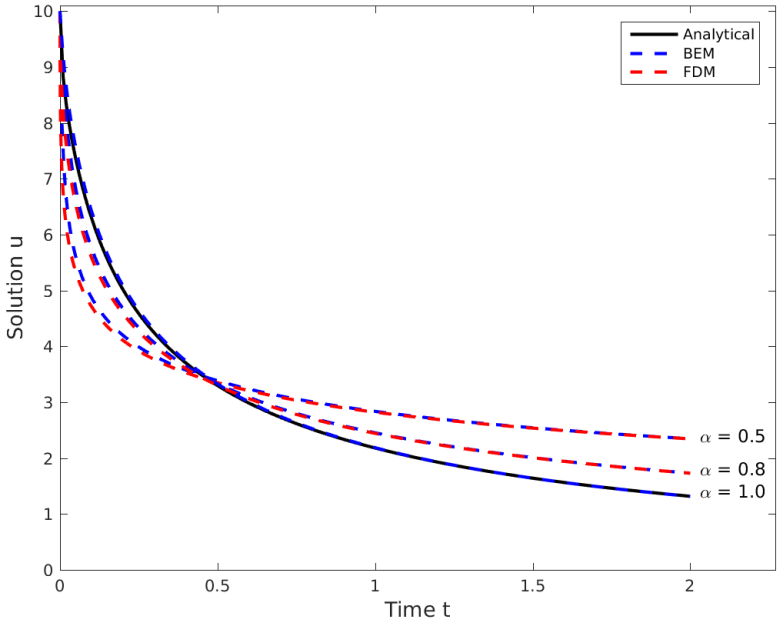

Figure 4.22: Square domain: results $u(L/2, L/2, t)$ for the anisotropic medium.

described in the polar coordinate system (r, θ); thus, this problem is defined in the domain: $0 \leq r \leq R, 0 \leq \theta \leq 2\pi$.

We assume the problem to be fully axisymmetric, so the solution is independent of the angular coordinate θ, allowing the governing PDE (2.1) to be rewritten as:

$$\frac{\partial^\alpha u}{\partial t^\alpha} = D\left(\frac{\partial^2 u}{\partial r^2} + \frac{1}{r}\frac{\partial u}{\partial r}\right), \quad 0 < \alpha < 1 \tag{4.15}$$

If the problem to be solved has a zero initial condition $u(r, \theta, 0) = 0$, and is subject to a boundary condition

$$u(R, \theta, t) = \hat{u} \tag{4.16}$$

then the analytical solution u_{an} for the case $\alpha = 1$ is that given by Greenberg [36] as

$$u_{an}(r, t) = \hat{u} - \frac{2\hat{u}}{R}\sum_{n=1}^{\infty}\frac{J_0(\lambda_n r)}{\lambda_n J_1(\lambda_n R)}\mathrm{e}^{-D\lambda_n^2 t} \tag{4.17}$$

where $J_0(\cdot)$ and $J_1(\cdot)$ are Bessel functions of the first kind and orders zero and one, respectively, and the parameters λ_n are the positive roots of the equation

$$J_0(\lambda_n R) = 0 \tag{4.18}$$

The analyses were carried out with the parameters $D = 1, R = 10$ and $\hat{u} = 10$. Three meshes were employed to investigate the convergence of the BEM results to the analytical solution. The first mesh, depicted in Figure 4.23, has $n_\Gamma = 16$ and $n_\Omega = 144$. The second mesh was generated by refining the angular and radial discretisation of the first mesh. It has $n_\Gamma = 32$ and $n_\Omega = 544$, and is depicted in Figure 4.24. The third mesh was generated by following the same procedure and is of size $n_\Gamma = 64$ and $n_\Omega = 2368$, as shown in Figure 4.25. These meshes will be called, respectively, mesh 1, 2 and 3.

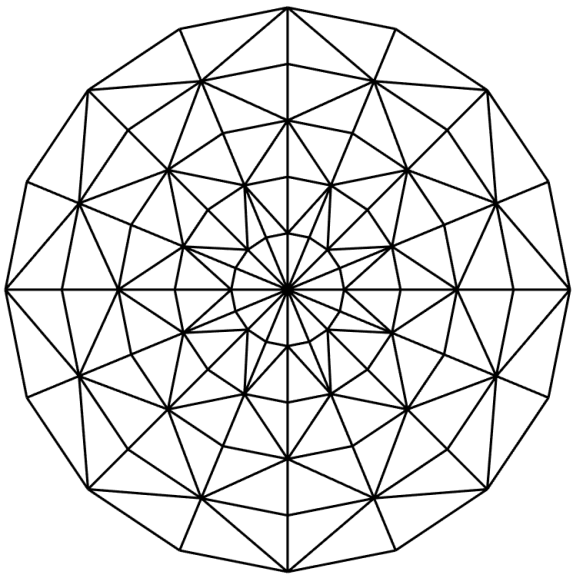

Figure 4.23: BEM mesh 1 for the circular domain

The convergence of the BEM results to the analytical solution can be studied through the computation of the relative L^2 error norm, E_2, from (4.11). For the case $\alpha = 1$, we take the reference solution $u_{ref} = u_{an}$

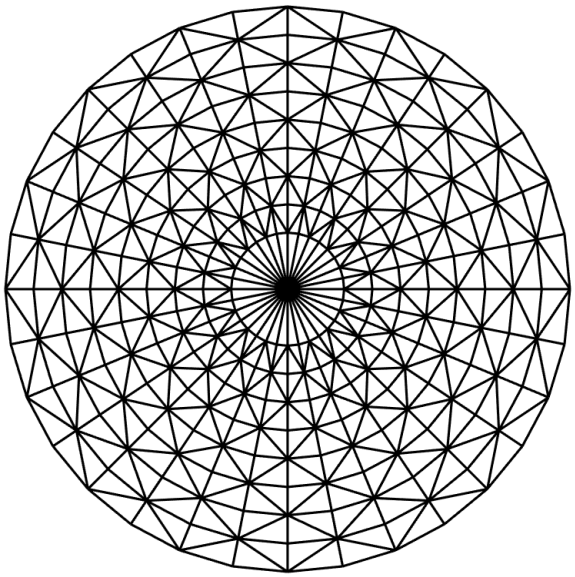

Figure 4.24: BEM mesh 2 for the circular domain

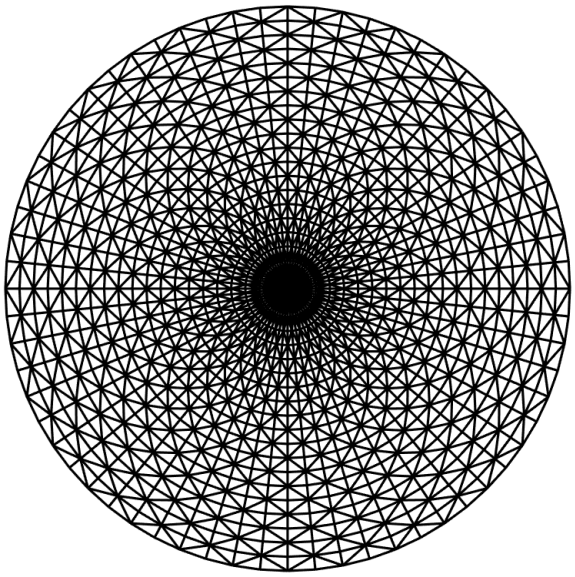

Figure 4.25: BEM mesh 3 for the circular domain

from (4.17). Figure 4.26 presents the results for the error norm E_2 at $t = 4$, 8, 12, and 20, obtained with $\Delta t = 0.8$ for mesh 1, $\Delta t = 0.4$ for mesh 2, and $\Delta t = 0.2$ for mesh 3. The model refinement produces a reduction in the error, verifying the convergence of the numerical results to the analytical solution. It is also noticeable that larger errors are found at the beginning of the analysis, but as time increases and the problem approaches the steady-state condition, the errors reduce.

A comparison between analytical and BEM results, obtained with mesh 3, at selected instants of time, is shown in Figure 4.27. Good agreement is observed between them, with only minor discrepancies at the early times $t = 1, 4$ at coordinates $r < 5$. This observation is in agreement with Figure 4.26, which shows larger errors at the beginning of the analysis.

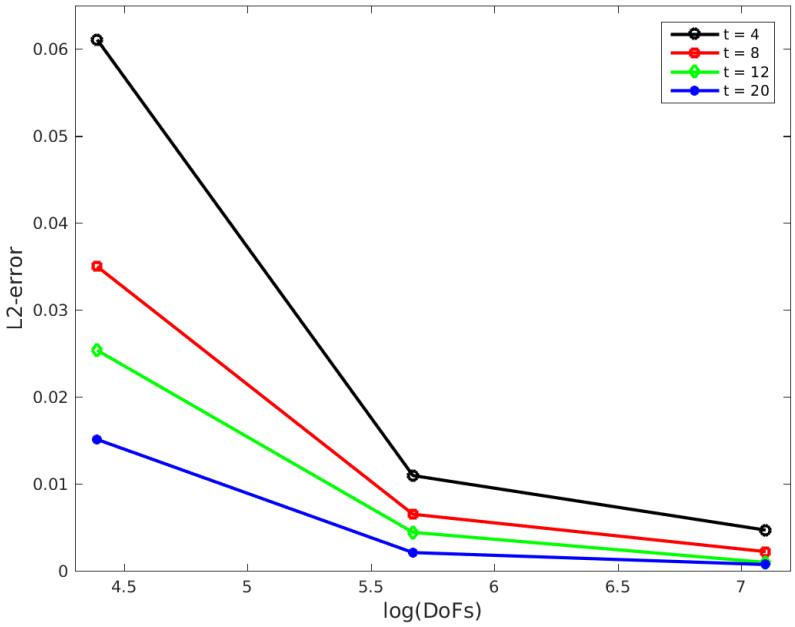

Figure 4.26: Circular domain: convergence for case $\alpha = 1$.

In the absence of an analytical solution for the case $\alpha \neq 1$, we make use of the fact that this is an axisymmetric problem and take our reference solution to be the results of a refined axisymmetric finite difference scheme which requires discretisation only in the radial direction. For our BEM analysis for the case $\alpha = 0.8$, we adopt time steps $\Delta t = 0.4, 0.2, 0.1$ for meshes 1, 2, 3 respectively. The corresponding time steps for the case $\alpha = 0.5$ are $\Delta t = 0.1, 0.05, 0.025$. The convergence of the BEM scheme for these two values of α is presented in Figures 4.28 and 4.29.

The evolution of u over a radial cross section with time is shown in Figures 4.30 and 4.31 for the cases $\alpha = 0.8, 0.5$ respectively. As for the case $\alpha = 1$, only minor discrepancies with the reference solution are seen at early times, t, and for small r.

The results at $r = 2, 4, 6, 8$, as a function of time, are depicted in Figure 4.32 for the case $\alpha = 1$ and show excellent agreement with the analytical solution. Similar plots (not shown for reasons of brevity) demonstrate similar congruence with the reference solution for the cases $\alpha = 0.8$ and $\alpha = 0.5$.

5 Conclusions

The main novelty of this work is the D-BEM formulation developed for the solution of the anomalous diffusion equation. The formulation was developed using the Riemann-Liouville operator, with the integral

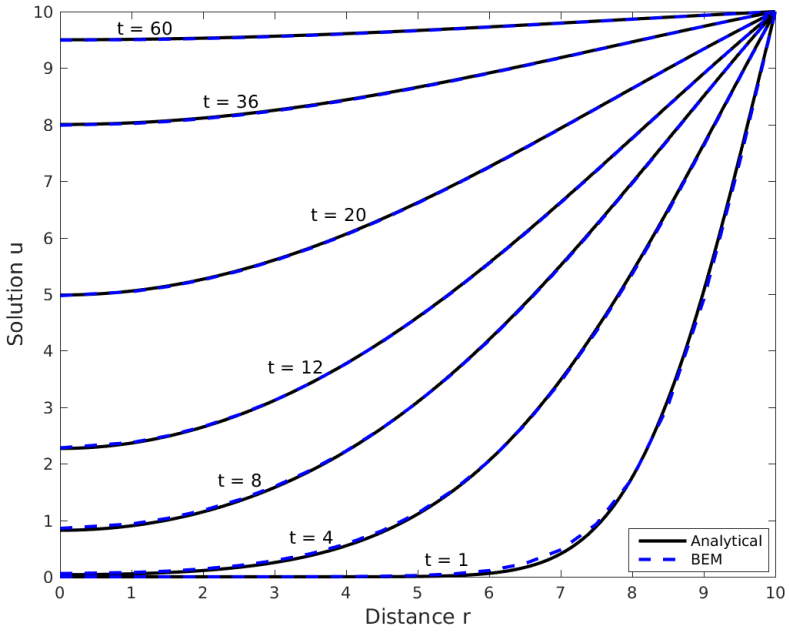

Figure 4.27: Circular domain: evolution of results with time, $\alpha = 1$.

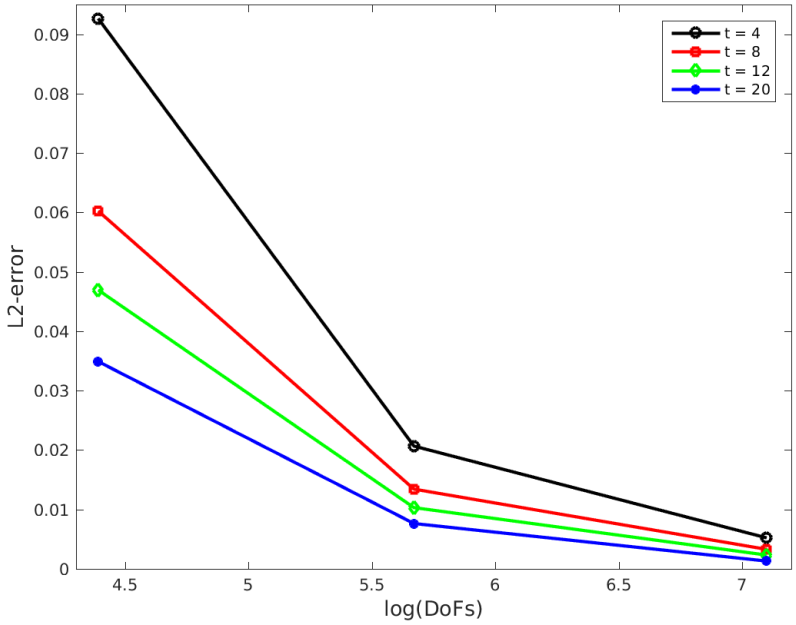

Figure 4.28: Circular domain: convergence for case $\alpha = 0.8$.

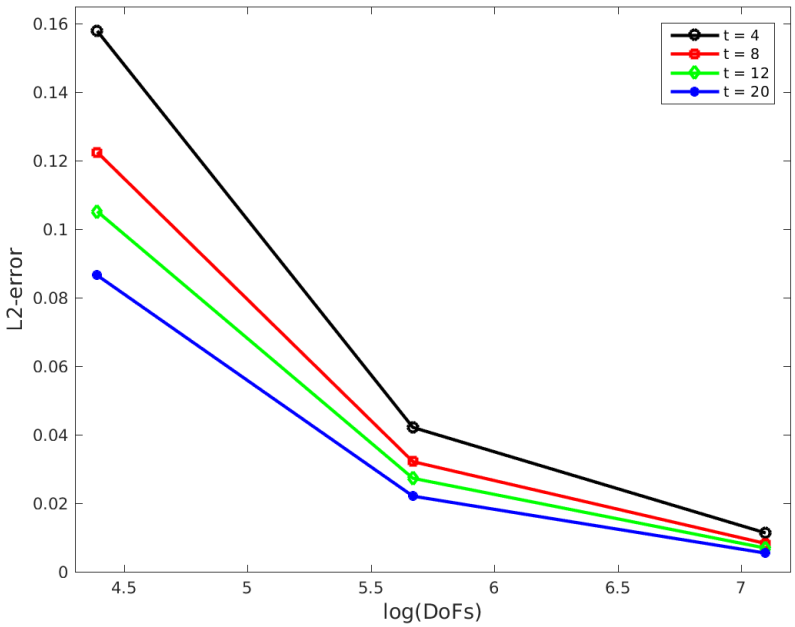

Figure 4.29: Circular domain: convergence for case $\alpha = 0.5$.

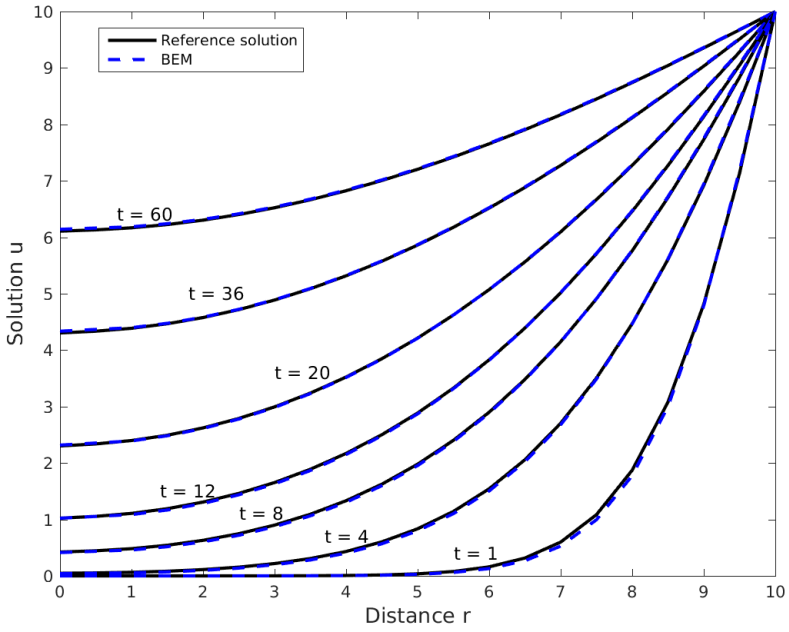

Figure 4.30: Circular domain: evolution of results u on a radial section, $\alpha = 0.8$.

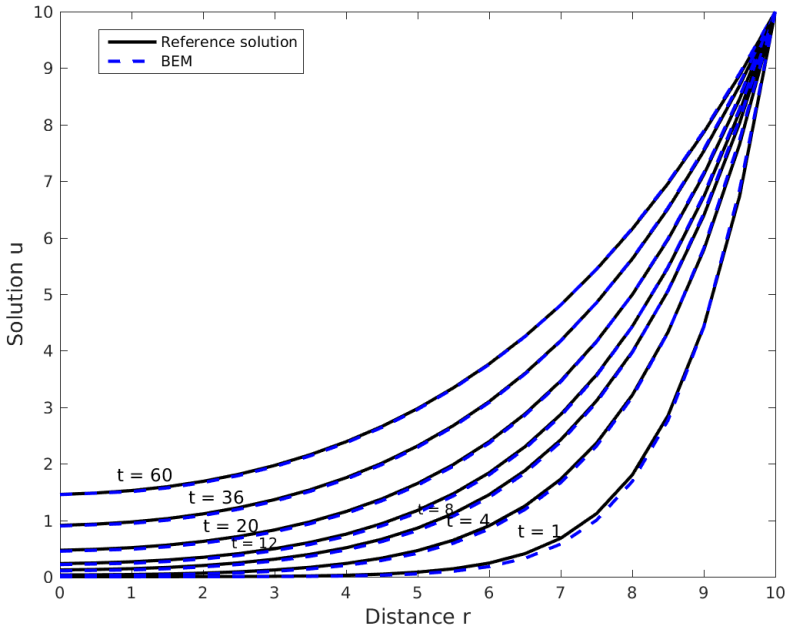

Figure 4.31: Circular domain: evolution of results u on a radial section, $\alpha = 0.5$.

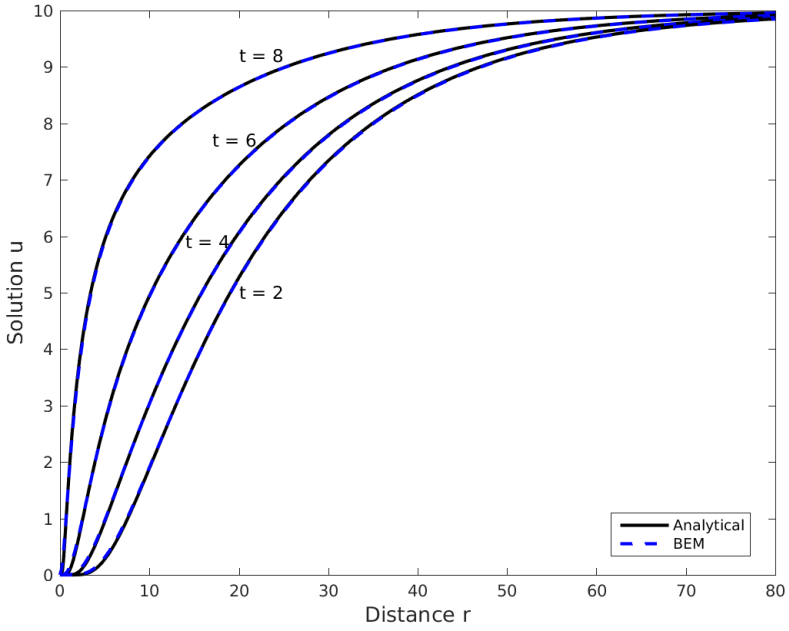

Figure 4.32: Circular domain: evolution of results with time.

that appears in this operator being computed under the assumption that the variable of interest and its normal derivative are constant within each time step. The formulation is capable of providing reliable results for values of the fractional derivative of order $\alpha \geq 0.5$. In the second example, we present results for $\alpha = 0.2$. However, for values of $\alpha < 0.5$ small time steps are required to capture the large temporal gradients in the solution immediately after $t = 0$, causing the analysis to become time-consuming. As a suggestion to overcome such a difficulty, the use of variable time steps seems to be very promising: beginning the analysis with very small values, greater values can be used as the time increases, in order to improve the computational efficiency. Another approach might be the use of more sophisticated interpolation functions.

Notwithstanding the above comments relating to computational efficiency for small α, it has been demonstrated that the D-BEM formulation is capable of producing accurate results for problems of anomalous diffusion characterised by governing PDEs containing a fractional calculus operator. The formulation has been shown to produce results of high accuracy, outperforming a finite difference approximation.

References

[1] K.S. Miller and B. Ross. *An Introduction to the Fractional Calculus and Fractional Differential Equations*. Wiley-Interscience, 1993.

[2] M.D. Ortigueira. *Fractional Calculus for Scientist and Engineers. Lecture Notes in Electrical Engineering, volume 84*. Springer, 2011.

[3] H. El-Saka and E. Ahmed. A fractional order network model for ZIKA. *bioRxiv*, DOI:http://dx.doi.org/10.1101/039917, 2016.

[4] W. Cai, W. Chen, and W. Xu. Fractional modeling of Pasternak-type viscoelastic foundation. *Mechanics of Time-Dependent Materials*, 21:119–131, 2017.

[5] G. Moradi and B. Mehdinejadiani. Modeling solute transport in homogeneous and heterogeneous porous media using spatial fractional advection-dispersion equation. *Soil and Water Research*, 13:18–28, 2018.

[6] H. Sun, Y. Zhang, D. Baleanu, W. Chen, and Y. Chen. A new collection of real world applications of fractional calculus in science and engineering. *Communications in Nonlinear Sciences and Numerical Simulation*, 64:213–231, 2018.

[7] M.M. Meerschaert and C. Tadjeran. Finite difference approximations for fractional advection-dispersion flow equations. *Journal of Computational and Applied Mathematics*, 172:65–77, 2004.

[8] J.Q. Murilo and S.B. Yuste. An explicit difference method for solving fractional diffusion and diffusion-wave equations in the Caputo form. *Journal of Computational and Nonlinear Dynamics*, 6, 2011.

[9] C. Li, Z. Zhao, and Y.Q. Chen. Numerical approximation of nonlinear fractional differential equations with subdiffusion and superdiffusion. *Computers and Mathematics with Applications*, 62:855–875, 2011.

[10] C. Celic and M. Duman. Crank-Nicolson method for the fractional diffusion equation with the Riesz fractional derivative. *Journal of Computational Physics*, 231:1743–1750, 2012.

[11] W. Li and C. Li. Second order explicit difference schemes for the space fractional advection diffusion equation. *Applied Mathematics and Computations*, 257:446–457, 2015.

[12] E. Sousa and C. Li. A weighted Finite Difference Method for the fractional diffusion equation based on the Riemann-Liouville derivative. *Applied Numerical Mathematics*, 90:22–37, 2015.

[13] C. Tadjeran and M.M. Meerschaert. A second-order accurate numerical method for the two-dimensional fractional diffusion equation. *Journal of Computational Physics*, 220:813–823, 2007.

[14] D.A. Murio. Implicit finite difference approximation for time fractional diffusion equations. *Computers and Mathematics with Applications*, 56:1138–1145, 2008.

[15] S.B. Yuste and L. Acedo. An explicit Finite Difference Method and a new von Neumann-type stability analysis for fractional diffusion equations. *SIAM Journal on Nmerical Analysis*, 42:1862–1874, 2005.

[16] O.P. Agrawal. A general finite element formulation for fractional variational problems. *Journal of Mathematical Analysis and Applications*, 337:1–12, 2008.

[17] Y. Zheng, C. Li, and Z. Zhao. A note on finite element method for the space-fractional advection diffusion equation. *Computers and Mathematics with Applications*, 59:1718–1726, 2010.

[18] W.H. Deng. Finite element method for the space and time fractional Fokker-Planck equation. *SIAM Journal on Numerical Analysis*, 47:204–226, 2008.

[19] J.P. Roop. Computational aspects of FEM approximation of fractional advection dispersion equations on bounded domains in $\mathbb{R}^2$. *Journal of Computational and Applied Mathematics*, 193:243–268, 2006.

[20] Q. Huang, G. Huang, and H. Zhan. A finite element solution for the fractional advection-dispersion equation. *Advances in Water Resources*, 31:1578–1589, 2008.

[21] M. Dehghan and M. Safarpoor. The dual reciprocity Boundary Elements Method for the linear and nonlinear two-dimensional time-fractional partial differential equations. *Mathematical Methods in the Applied Sciences*, 39:3979–3995, 2016.

[22] J.T. Katsikadelis. The BEM for numerical solution of partial fractional differential equations. *Computers and Mathematics with Applications*, 62:891–901, 2011.

[23] F.S. Zafarghandi, M. Mohammadi, E. Babolian, and S. Javadi. Radial basis functions method for solving the fractional diffusion equations. *Applied Mathematics and Computation*, 342:224–246, 2019.

[24] A. Shirzadi, L. Ling, and S. Abbasbandy. Meshless simulations of the two-dimensional fractional-time convection-diffusion-reaction equations. *Engineering Analysis with Boundary Elements*, 36:1522–1527, 2012.

[25] W.J. Mansur. *A Time-Stepping Technique to Solve Wave Propagation Problems Using the Boundary Element Method*. Ph.D. Thesis, University of Southampton, 1983.

[26] L.C. Wrobel. *Potential and Viscous Flow Problems Using the Boundary Element Method*. Ph.D. Thesis, University of Southampton, 1981.

[27] C.A. Brebbia, J.C.F. Telles, and L.C. Wrobel. *Boundary Element Techniques: Theory and Application in Engineering*. Springer Verlag, 1984.

[28] O.C Zienkiewicz and K. Morgan. *Finite Elements & Approximation*. John Wiley & Sons, New York, 1983.

[29] G.D. Smith. *Numerical solution of partial differential equations: Finite Difference Methods*. Clarendon Press, Oxford, 1985.

[30] J.R. Berger and A. Karageorghis. The Method of Fundamental Solutions for heat conduction in layered materials. *International Journal for Numerical Methods in Engineering*, 45:1681–1694, 1999.

[31] J.A.M. Carrer, C.L.N. Cunha, and W.J. Mansur. The Boundary Element Method applied to the solution of two-dimensional diffusion-advection problems for non-isotropic materials. *Journal of the Brazilian Society of Mechanical Sciences and Engineering*, 39:4533–4545, 2017.

[32] S.S. Ray. Exact solutions for time-fractional diffusion-wave equations by decomposition method. *Physica Scripta*, 75:53–61, 2007.

[33] H.J. Haubold, A.M. Mathai, and R.K. Saxena. Mittag-Leffler functions and their applications. *Journal of Applied Mathematics*, 2011.

[34] Y. Ochiai, V. Sladek, and J. Sladek. Transient heat conduction analysis by triple-reciprocity Boundary Element Method. *Engineering Analysis with Boundary Elements*, 30:194–204, 2006.

[35] J.A.M. Carrer, M.F. Oliveira, R.J. Vanzuit, and W.J. Mansur. Transient heat conduction by the Boundary Element Method. *International Journal for Numerical Methods in Engineering*, 89:897–913, 2012.

[36] M.D. Greenberg. *Advanced Engineering Mathematics*. Prentice-Hall, New Jersey, 1998.